

TPRL



THERMOPHYSICAL PROPERTIES RESEARCH LABORATORY

AFOSR-TR- 84 - 0869

TPRL 406

THERMOPHYSICAL PROPERTY TESTING USING TRANSIENT TECHNIQUES

Final Report on Contract F 49620-81-K0011

to the

Air Force Office of Scientific Research

by

R.E. Taylor, R.L. Shoemaker, J.A. Stark and L.G. Koshigoe

DTIC
SELECTE
NOV 1 1984
D

June 1984

School of Mechanical Engineering

Purdue University, West Lafayette, Indiana

Approved for public release
distribution unlimited.

84 - 0869

AD-A147 085

DTIC FILE COPY

THERMOPHYSICAL PROPERTIES RESEARCH LABORATORY

School of Mechanical Engineering

Purdue University
2595 Yeager Road
W. Lafayette, IN 47906
(317) 463-1581

R.E. Taylor:	Director and Senior Researcher
R.L. Shoemaker:	Assistant Director and Associate Senior Researcher
H. Groot:	Engineering Associate
W. Vaughn:	Engineering Technical Associate
T. Goerz:	Computer Programmer
J. Larimore:	Secretary

UNCLASSIFIED

SECURITY CLASSIFICATION OF THIS PAGE (When Data Entered)

REPORT DOCUMENTATION PAGE		READ INSTRUCTIONS BEFORE COMPLETING FORM
1. REPORT NUMBER AFOSR-TR- 84-0869	2. GOVT ACCESSION NO. <i>AD A 085</i>	3. RECIPIENT'S CATALOG NUMBER
4. TITLE (and Subtitle) "Thermophysical Property Testing Using Transient Techniques"		5. TYPE OF REPORT & PERIOD COVERED FINAL SCIENTIFIC REPORT 2/1/81 - 5/1/84
7. AUTHOR(s) R.E. Taylor, R.L. Shoemaker, J.A Stark and L.G. Koshigoe		6. PERFORMING ORG. REPORT NUMBER TPRL 406
9. PERFORMING ORGANIZATION NAME AND ADDRESS Thermophysical Properties Research Laboratory Purdue University West Lafayette, IN 47906		8. CONTRACT OR GRANT NUMBER(s) F 49620-81-K0011
11. CONTROLLING OFFICE NAME AND ADDRESS Air Force Office of Scientific Research, <i>NA</i> Bolling AFB, D.C. 20332 - 2442		10. PROGRAM ELEMENT, PROJECT, TASK AREA & WORK UNIT NUMBERS <i>61102F</i> <i>2307 A1</i>
14. MONITORING AGENCY NAME & ADDRESS (if different from Controlling Office)		12. REPORT DATE 6/29/84
		13. NUMBER OF PAGES 46
		15. SECURITY CLASS. (of this report) UNCLASSIFIED
		15a. DECLASSIFICATION/DOWNGRADING SCHEDULE
16. DISTRIBUTION STATEMENT (of this Report) Approved for public release - distribution unlimited		
17. DISTRIBUTION STATEMENT (of the abstract entered in Block 20, if different from Report)		
18. SUPPLEMENTARY NOTES		
19. KEY WORDS (Continue on reverse side if necessary and identify by block number) Specific heat HMX carbon/carbon Diffusivity RDX solid propellants Conductivity AP HTPB		
20. ABSTRACT (Continue on reverse side if necessary and identify by block number) Transient techniques were applied to the study of energetic materials (AP, HMX, RDX and HTPB) used in solid rocket fuel to carbon/carbon materials used as rocket nozzles. Studies on AP included single crystals, pressed powders and AP/HTPB mixtures. It was found that the conductivity of AP can be considered isotropic, even in the orthorhombic phase. The conductivity values for pure AP calculated from the AP/HTPB mixtures were somewhat larger than those measured directly on single crystals due to imperfections in the relatively large single crystals. Conductivity values for Beta HMX obtained on pressed powders are be-		

lieved to be 20% below those that would be obtained on good single crystals if they were available. Delta phase values are believed representative. Conductivity data useful for modeling AP/binder and HMX/binder fuel from RT to combustion were obtained.

Successful techniques for determining in-situ conductivity values for carbon fibers and matrix in c/c composites were developed. The relative roles of the fibers and matrix in c/c subject to transient heat fluxes were delineated. The advantages of off-axis testing were revealed. Diffusivity values corresponding to thermal conductivity results could be obtained. The presence of a surface layer in which interconstituent thermal gradients are important and beyond which they are negligible was demonstrated.

Accession For	
NTIS GPO	<input checked="" type="checkbox"/>
DTIC TAB	<input type="checkbox"/>
Unannounced	<input type="checkbox"/>
Justification	
By _____	
Distribution/	
Availability Codes	
Dist	Avail and/or Special
A/1	



TABLE OF CONTENTS

	<u>Page</u>
1.0 INTRODUCTION	1
1.1 Background	1
1.2 Objectives	1
2.0 MATERIAL DESCRIPTIONS	3
2.1 Energetic Materials	3
2.1 a Background	3
2.1 b Sample Description	5
2.2 Carbon/Carbon Materials	10
3.0 RESULTS	13
3.1 Energetic Materials	13
3.1 a Modifications to Existing Techniques	13
3.1 b Examination of Alternate Techniques	14
3.1 c Influence of Optical Properties on Diffusivity Measurements	15
3.1 d Specific Heat	16
3.1 e Thermal Diffusivity	16
3.1 f Thermal Conductivity	24
3.2 Carbon/Carbon Materials	32
4.0 DISCUSSION	32
4.1 Energetic Materials	32
4.1 a AP	32
4.1 b HMX and RDX	35
4.2 Carbon/Carbon Materials	36
5.0 SUMMARY AND CONCLUSIONS	37
6.0 REFERENCES	39
APPENDICES	42
I. Publications, Presentations and Reports	42
II. Tabulated Values	45

AIR FORCE OFFICE OF SCIENTIFIC RESEARCH (AFOSR)
NOTICE OF TRANSFERENTIAL TO DTIC
This technical report has been reviewed and approved for public release under E.O. 13526-12.
Distribution is unlimited.
MATTHEW J. KEEFER
Chief, Technical Information Division

LIST OF TABLES

	<u>Page</u>
1. AP Crystal Diffusivity Samples	8
2. AP Powder Diffusivity Samples	8
3. AP/HTPB Diffusivity Samples	8
4. HMX Diffusivity Samples	9
5. RDX Diffusivity Samples	9
6. Sample Geometries and Bulk Density Values of C/C Samples	12
7. Measured Unit Cell Dimension (mm) and Calculated Yarn Bundle Fractions for On-Yarn Diffusivity Specimens from O.D. Region of Billet F-11	12
8. Thermal Diffusivity Values for a Fiber Bundle Experiment	33

LIST OF FIGURES

1. Isotherms in Sample Cups	6
2. Crystal Structure of AP	7
3. Nomenclature for 3-D Cylindrical Unit Cell and Sketch Showing Five Directions in Which Diffusivity was Measured	11
4. Specific Heat	17
5. Thermal Diffusivity of AP Single Crystal	18
6. Thermal Diffusivity of AP/HTPB	20
7. Thermal Diffusivity of HMX-2	21
8. Thermal Diffusivity of HMX	22
9. Thermal Diffusivity of RDX	23
10. Thermal Conductivity of Single Crystal AP	25
11. Thermal Conductivity of AP/HTPB	26
12. Thermal Conductivity of AP Calculated from AP/HTPB Data	28
13. Thermal Conductivity of AP	29
14. Thermal Conductivity of HMX	30
15. Thermal Conductivity of RDX	31
16. Normalized Rear Face Temperature Rise for Axial-Circumferential Sample at 552°C	34

THERMOPHYSICAL PROPERTY DETERMINATIONS USING TRANSIENT TECHNIQUES

1.0 INTRODUCTION

1.1 Background

In order to model the complex combustion process of solid rocket fuels, knowledge of their thermophysical properties and behavior under transient temperature conditions up to decomposition or melting is required. Studies of thermophysical properties by transient techniques is particularly useful for materials involved in rocket propulsion. This is true for both the energetic materials used as fuel and for the composite materials used as rocket nozzles and exit cones. The energetic materials are by their very nature unstable so that methods which utilize small samples and fast measurement times are obviously superior to the more traditional techniques. Measurements can be made in unstable regions so that knowledge of the property changes which will occur in the actual operating environment can be obtained. Of course, enhanced safety is inherent with the use of smaller samples.

In addition, we have shown previously that transient techniques can be very powerful tools in studying heat flow through fiber-reinforced composites. One can gain information on the relative roles of the reinforcements and the matrices during transients that simply cannot be obtained by other techniques.

1.2 Objectives

The primary purposes of this research were to understand thermophysical properties of ammonium perchlorate (AP), cyclotetramethylene tetranitramine (HMX), cyclotrimethylene trinitramine (RDX), and hydroxy-terminated polybutadiene (HTPB, used as a binder) up to their destruction/melting temperature and to further the understanding of transient heat flow in carbon/carbon materials used as rocket nozzles. The research on carbon/carbon materials was funded only for the first year of the grant.

The general approach used was to examine the specific heats (C_p) using a Perkin-Elmer Model DSC II and the thermal diffusivity (α) using the laser flash method. From these properties, the behavior of the thermal conductivity (λ) can be calculated since $\lambda = \alpha C_p d$ where d is the density. This approach has the advantage of separating the thermal conductivity into a thermodynamic part (C_p and d) and a transport part (α). Thermodynamic properties are relatively well-behaved and understood so the present results could be interpreted readily and extrapolated confidently as required. Thus a major portion of the program could be devoted to thermal diffusivity studies, which are inherently simpler experiments than thermal conductivity studies.

In order to accomplish these objectives for the energetic materials, the following goals had to be attained:

- (a) - The modification of present instrumentation to allow the measurement of the specific heat and the thermal diffusivity of energetic materials.
- (b) - The examination of alternate methods for determining the thermophysical properties.
- (c) - The examination of the optical properties of the energetic materials in the infrared region, to determine if an IR detector can see into the material in its different forms; e.g. single crystal and pressed powder.
- (d) - The determination of each material's specific heat in its different phases.
- (e) - The examination of the specific heat measurement's heating rate sensitivity for the various materials.
- (f) - An examination of how sensitive the specific heat is to decomposition products within the sample.
- (g) - The determination of each material's thermal diffusivity up to decomposition, using the best pure samples obtainable.

- (h) - The examination of the sensitivity of the thermal diffusivity to decomposition products and sample changes as a results of decomposition.
- (i) - The determination of the thermophysical properties of a binder.
- (j) - The determination of the thermal diffusivity of mixtures of oxidizer plus binder and comparison to the results of computations based on the constituent properties.

In order to accomplish the objective for the carbon/carbon materials, the following goals had to be accomplished:

- (a) - Explore the problems associated with transient temperature measurements of the rear surface of a fiber-reinforced composite including spot size and use of localized sensors.
- (b) - Develop techniques to determine the in-situ diffusivity values for fibers.
- (c) - Examine the overall concept of diffusivity applied to fiber-reinforced materials.
- (d) - Determine the relationship between the diffusivity values for the constituents and the effective value for the composite.
- (e) - Examine the merits of off-axis testing.

2.0 MATERIAL DESCRIPTION

2.1 Energetic Materials

2.1 a Background

Ammonium perchlorate has two solid state phases important to rocket applications. Phase II exists from -190°C to 240°C . Its crystal lattice is orthorhombic $Pnma$ ($a = 0.202\text{\AA}$, $b = 5.816\text{\AA}$, $c = 7.449\text{\AA}$). This phase has four molecules per unit cell of the lattice, giving it a density of 1.957 g/cm^3 . Phase II exists from 240°C to 450°C (the melting point). Its lattice is cubic $F\bar{4}3m$ ($a = 7.53\text{\AA}$). This phase also has four molecules per unit cell. Its density is 1.756 g/cm^3 [1-3]. Significant decompo-

sition of AP begins around 202°C [4-5].

RDX is a relatively unstable material. It begins to decompose and melt around 204°C. It has only one stable solid phase, the α -phase, in which the hexagonal ring molecule is in a "chair" configuration. The crystal lattice is orthorhombic $Pbca$ ($a = 13.18\text{\AA}$, $b = 11.57\text{\AA}$, $c = 10.71\text{\AA}$). There are eight molecules per unit cell and the density is 1.806 g/cm^3 . The β -phase can only be made to exist for short times at elevated temperatures [6-7].

HMX exists in two stable solid phases that are of importance to propellant studies [8-10]. The β -phase is stable from room temperature to 145°C. In this phase the octagonal ring molecule is in a "chair" shape and the crystal lattice is monoclinic $P2_1/c$ ($a = 6.54\text{\AA}$, $b = 11.05\text{\AA}$, $c = 8.70\text{\AA}$, $\beta = 124.3^\circ$). There are two molecules per unit cell, and the density is 1.90 g/cm^3 . The δ -phase normally exists from 156°C to the melting point at 279°C, however, decomposition begins to occur around 220°C. The δ -phase is of the hexagonal $P6_1$ structure ($a = 7.71\text{\AA}$, $c = 32.55\text{\AA}$), and the molecule is in a "boat" configuration. There are six molecules per unit cell in the δ -phase, and the density is 1.78 g/cm^3 .

Sample materials were acquired from several sources. AP and RDX pressed powders were obtained from Morton-Thiokol, Huntsville. The AP powder was $17.1\mu\text{m}$ grains, and RDX powder was a blend of 50% $16.0\mu\text{m}$ (Holston-lot #5775) 30% $6.0\mu\text{m}$ (Holston-lot #7017) and 20% $2.6\mu\text{m}$ (Holston-lot #5789) grains. HMX powder was from Morton-Thiokol, Huntsville and from Naval Weapons Center. Morton-Thiokol-supplied HMX was a blend of 50% $18.9\mu\text{m}$ (Holston-lot #5486), 30% $6.0\mu\text{m}$ (Holston-lot #7016), and 20% $3.3\mu\text{m}$ (Holston-lot #7016) grains. AP single crystals were from Naval Weapons Center. Premixed AP/HTPB binder materials were from Rocket Engineering, Seymore, IN. Samples were made from pure HTPB binder and several mixtures of binder and $200\mu\text{m}$ AP particles.

To make a diffusivity sample of one of the powdered materials, the powder was pressed into a stainless steel cup. The bottom of this cup was to serve as the sample front layer. However, finite element analyses of this cup design showed that the cup side wall would act as a heat sink, creating highly two-dimensional heat flow in the powder. Figure 1 shows a plot of finite-element-generated isotherms in the cup model after

the laser has flashed the cup bottom. To reduce the heat sink presence of the cup walls a new cup design was analyzed. The bottom surface of this new cup was stainless steel, but the walls were made of teflon, which has a diffusivity comparable to those of the powders being measured. A finite element analysis of the teflon cup model is included in Figure 1. The isotherms shown here represent a heat flow that is very nearly one dimensional throughout the measurement duration. Based on this analysis, it was decided that the teflon cup samples would be made and used.

2.1 b Sample Description

Several single crystals of 99.999% pure AP were donated by T. Boggs of Naval Weapons Center. Since all of the large AP crystals were of the same shape, and they appeared similar to crystals studied by Kraeutle [11], all of the crystals were expected to have the same lattice orientation in relation to their observed shape. One of the large crystals was used for x-ray diffraction measurements to verify the crystal lattice orientation within the specimen. The diffraction sample could not be used for diffusivity measurements, as AP is very susceptible to x-ray induced lattice defects [12]. Therefore, the other crystals were used to make diffusivity samples. The crystals were large enough to allow cleavage of several diffusivity samples from each. Since cleavage of an AP crystal along planes perpendicular to each of its crystallographic axes is not easily accomplished, the cleavage planes used were those parallel to the natural growth surfaces of the crystals - these are the Miller planes $\langle 002 \rangle$, $\langle 2\bar{1}0 \rangle$ and $\langle 210 \rangle$. In the diffusivity samples these planes were made parallel to the sample faces. Therefore, diffusivities were measured perpendicular to the indicated Miller planes.

The $\langle 002 \rangle$ measurements were parallel to the crystallographic c-axis. The $\langle 210 \rangle$ and $\langle 2\bar{1}0 \rangle$ measurements were in directions which lay in the a-b plane (See Figure 2). Due to the symmetry of these two directions through the crystal structure, the set of two equations needed to resolve the diffusivities along the a- and b-axes became singular and could not be solved. Therefore, results are reported as

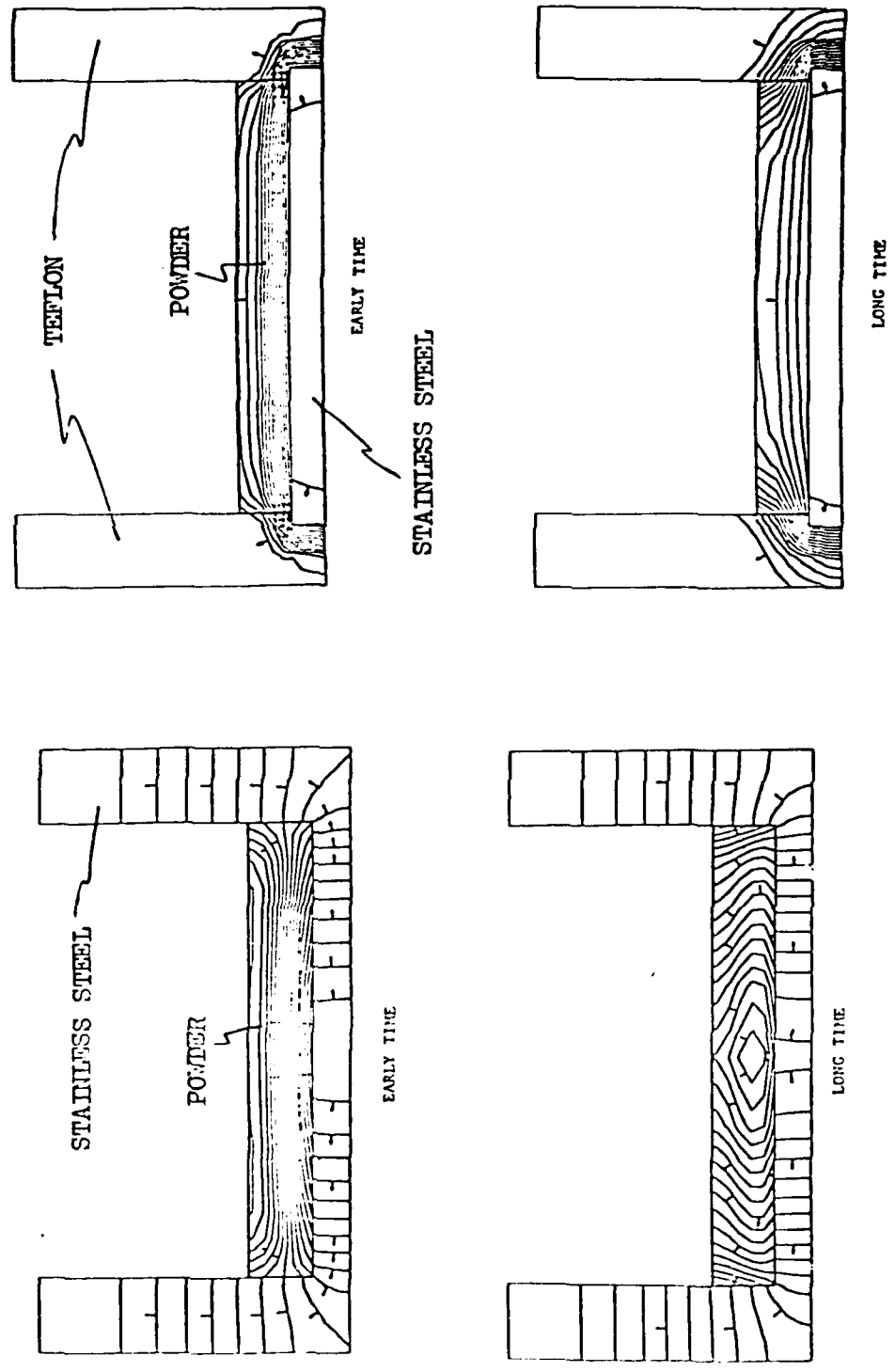


Figure 1. Isotherms in Sample Cups

diffusivities perpendicular to these planes, rather than parallel to the a- and b-axes. AP crystal samples are described in Table 1. In the sample designation, the first number indicates the large crystal from which a sample was cleaved. The second number identifies the actual sample.

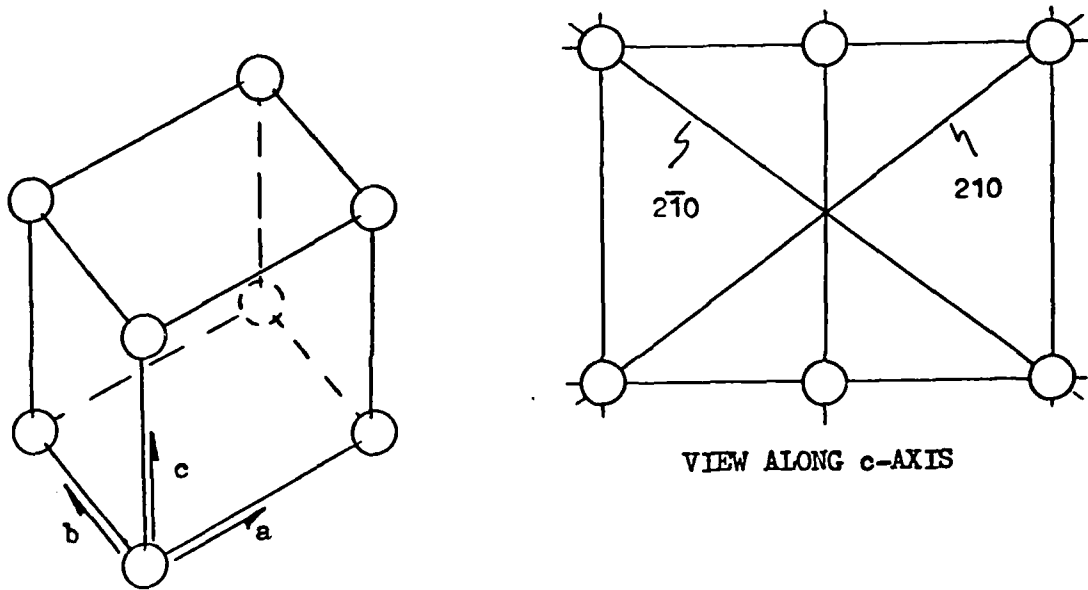


Figure 2. Crystal Structure of AP

Table 1. AP Crystal Diffusivity Samples

Sample	Miller Plane	Graphite Thickness (cm)	Crystal Thickness (cm)
2-5	<210>	0.0540	0.164
2-8	<210>	0.0557	0.152
3-2	<210>	0.0483	0.168
2-12	<210>	0.0529	0.151
3-3	<2 $\bar{1}$ 0>	0.0465	0.221
3-4	<2 $\bar{1}$ 0>	0.0479	0.214
3-5	<002>	0.0466	0.225
3-6	<002>	0.0483	0.277

To further characterize the AP, and allow comparison to RDX and HMX results, AP was also measured in pressed powder form. In addition, various mixtures of AP granules and HTPB binder were measured. Table 2 contains information about the AP powder samples and Table 3 describes the AP/HTPB diffusivity samples.

Table 2. AP Powder Diffusivity Samples

Sample	Powder Density (g/cm ³)	Front Layer Thickness (cm)	Rear Layer Thickness (cm)
24A	1.839	0.0780	0.1198
27A	1.839	0.0782	0.1196

Table 3. AP/HTPB Diffusivity Samples

Sample	AP Percent by Weight	AP Percent by Volume	Front Layer Thickness (cm)	Rear Layer Thickness (cm)
1-1	0	0	0.0543	0.142
3-1	70	51.8	0.0543	0.149
3-2	70	51.8	0.0524	0.116
4-2	80	64.8	0.0529	0.147
5-1	85	72.3	0.0557	0.144

HMX diffusivity samples are described in Table 4 and RDX diffusivity samples are described in Table 5.

Table 4. HMX Diffusivity Samples

Sample	Front Layer Material	Front Layer Thickness (cm)	Powder Thickness (cm)	Powder Density (g/cm ³)
HMX-1	SS 304	0.0782	0.1712	1.631
HMX-2	SS 304	0.0775	0.1312	1.655
3A	SS 304	0.0794	0.1208	1.608
9A	SS 304	0.0785	0.2077	1.630
11	Graphite	0.1809	0.1040	1.746

Table 5. RDX Diffusivity Samples

Sample	Powder Density (g/cm ³)	Front Layer Thickness (cm)	Powder Thickness (cm)
16A	1.540	0.0777	0.1425
19A	1.632	0.0787	0.2052
20A	1.572	0.0770	0.2085

2.2 Carbon/Carbon Material

A piece of carbon/carbon from billet F-11, from the 7-inch Mantech program [13] was used as the sample material. The piece was from Ring No. 17 near the outside diameter in the forward part of the billet [14]. The dimensions were 5.8 cm in the axial direction, 1.8 in the radial direction and 2.3 cm in the circumferential direction. Thermal diffusivity samples were machined in the axial (z), radial (r) and circumferential (θ) directions. In addition, samples were machined at 45° between the radial and axial direction (rz) and at 45° between the axial and circumferential directions ($z\theta$). The nomenclature and directions tested are shown in Figure 3. The sample dimensions, masses and bulk density values are listed in Table 6. Measured unit cell dimensions and calculated yarn bundle fractions for the principal axes are given in Table 7. Thus the actual yarn bundle fractions in the axial, radial and circumferential directions for these samples are 0.196, 0.067 and 0.277, respectively.

**Table 6. Sample Geometries and Bulk Density Values of
of C/C Samples**

Sample	Thick (in.)	Width (in.)	Width (in.)	Mass (gms)	Density (gms cm ⁻³)
Axial	0.3008	0.4728	0.5000	2.2308	1.914
Radial	0.2628	0.4990	0.5004	2.0430	1.900
Circumferential	0.2998	0.4906	0.5009	2.3017	1.907
Axial-Circumferential	0.3010	0.4993*	--	1.8672	1.934
Axial-Radial	0.2990	0.5000*	--	1.8590	1.932

*
Diameter

**Table 7. Measured Unit Cell Dimensions (mm) and Calculated Yarn
Bundle Fractions for On-Yarn Diffusivity Specimens
from O.D. Region of Billet F-11**

	Radial Sample	Axial Sample	Circ Sample
r_z	.41	-	-
r_θ	.81	-	-
z_r	-	.84	-
z_θ	-	1.67	-
C_r	-	-	1.07
C_z	-	-	.97
δ_r	-	2.18	2.29
δ_z	1.63	-	1.63
δ_θ	3.05	3.30	-
V_i	.067	.195	.277

1. Dimensions listed are averages of several measurements made on polished surface of the specimen with a calibrated-eyepiece microscope at 20X magnification.
2. Yarn bundle fractions calculated using relations of this type:

$$V_r = \frac{r_z r_\theta}{\delta_z \delta_\theta}$$

3.0 RESULTS

3.1 Energetic Materials

3.1 a Modifications of Existing Apparatuses

Due to the presence of volatile decomposition products it was necessary to modify the DSC apparatus for measuring C_p by adding a flow-through cover to remove contaminants. It was also necessary to modify the software program to allow the experimenter to change the end point to what it would have been in the absence of reaction/contamination when those processes are obviously going on at the end of the experiment. Since the beginning and end points are used to determine a reference line used in the calculations, the use of an erroneous end point negates the entire experiment. Erroneous end points are obtained when the conditions at the end of the heating cycle are not stable, i.e. decomposition is continuing at an appreciable rate or volatile contaminants are depositing on sensitive areas within the heating chamber. In this situation we have shown that it is still possible to salvage most of the data by adjusting the end point. The combined use of the flow-through cover and software modification has made possible the accurate determination of the specific heat of the energetic materials into the decomposition regions.

It was soon evident that the sharing of the existing laser flash diffusivity apparatus for both normal service activities and research on energetic materials was not very practical. The requirements for special sample holders, explosion containment, etc. dictated that a separate unit devoted to research be built. Fortunately, a second laser had been obtained from AFML. Thus it was necessary to build the containment system and a detector system consisting of a liquid-nitrogen cooled IR detector, appropriate lenses, biasing circuit, amplifiers, filters and A-to-D converter. With these components and the general up-grading of the laboratory data acquisition system, a separate flash diffusivity apparatus devoted to the study of energetic materials became available.

In order to obtain compacted powder samples of HMX, RDX and AP it was necessary to design cups suitable for pressing and transporting the samples. Our on-line capabilities for finite-element methods using in-house minicomputers for modeling heat flow through the cup-sample arrangement, was convenient.

In the case of free-standing samples, such as AP single crystals, binder, and binder plus AP powder, it was necessary to attach a graphite disk onto the front surface of the sample. The rear temperature transient was measured in the usual fashion and the diffusivity of the sample was calculated from our TWOLAYER program. These techniques were available at the start of the present research. However, the existing programs for heat-loss corrections were based on a single layer, so it was necessary to develop the mathematics for heat-loss corrections from composites consisting of two layers with grossly different properties.

The procedure for determining thermal diffusivity has been to allow the sample to come to thermal equilibrium at some temperature, then fire the laser and record the rear face temperature rise (normally one to two degrees), compute the diffusivity, increase the temperature to a new temperature and repeat the process. Since data could be obtained over a shorter time span if we did not equilibrate the sample temperature before each measurement, a technique was developed to increase the temperature at a constant rate and superimpose the laser firing on this ramp. Data analysis could be performed later. Using this technique, it was possible to obtain data over a temperature range of several hundred degrees in one-half to one-third the time required here-to-fore.

3.1 b Examination of Alternate Techniques for Determining Thermal Diffusivity

While it was recognized that the flash technique is capable of yielding the most accurate diffusivity values, it does suffer from the fact that even with ramping, many minutes are required for measuring values over a several hundred degree range. During this time period, samples of energetic materials will undergo decomposition. Thus, the

use of alternate techniques which are capable of much larger heating rates was explored. One obvious choice is placing the sample on thin ribbons of metal. The metal ribbons can be Joulean heated at very high rates. A simple apparatus was constructed and tested. The results are discussed in Report TPRL 300 (see List of Reports, Appendix I). The conclusion was that high accuracy could not be obtained in the case of very good thermal insulating materials since heat losses were comparable to heat entering the sample. Also, sample decomposition or melting would occur at the ribbon/sample interface in preference to heat flow through the sample, resulting in significant uncontrolled radiant heat from the sample's front surface. Thus, the choice seems to be between high accuracy, lower speed experiments and very low accuracy, high speed experiments. For reasons that will become obvious in the Discussion Section, we chose the high accuracy route.

3.1 c Influence of Optical Properties on Diffusivity Measurements

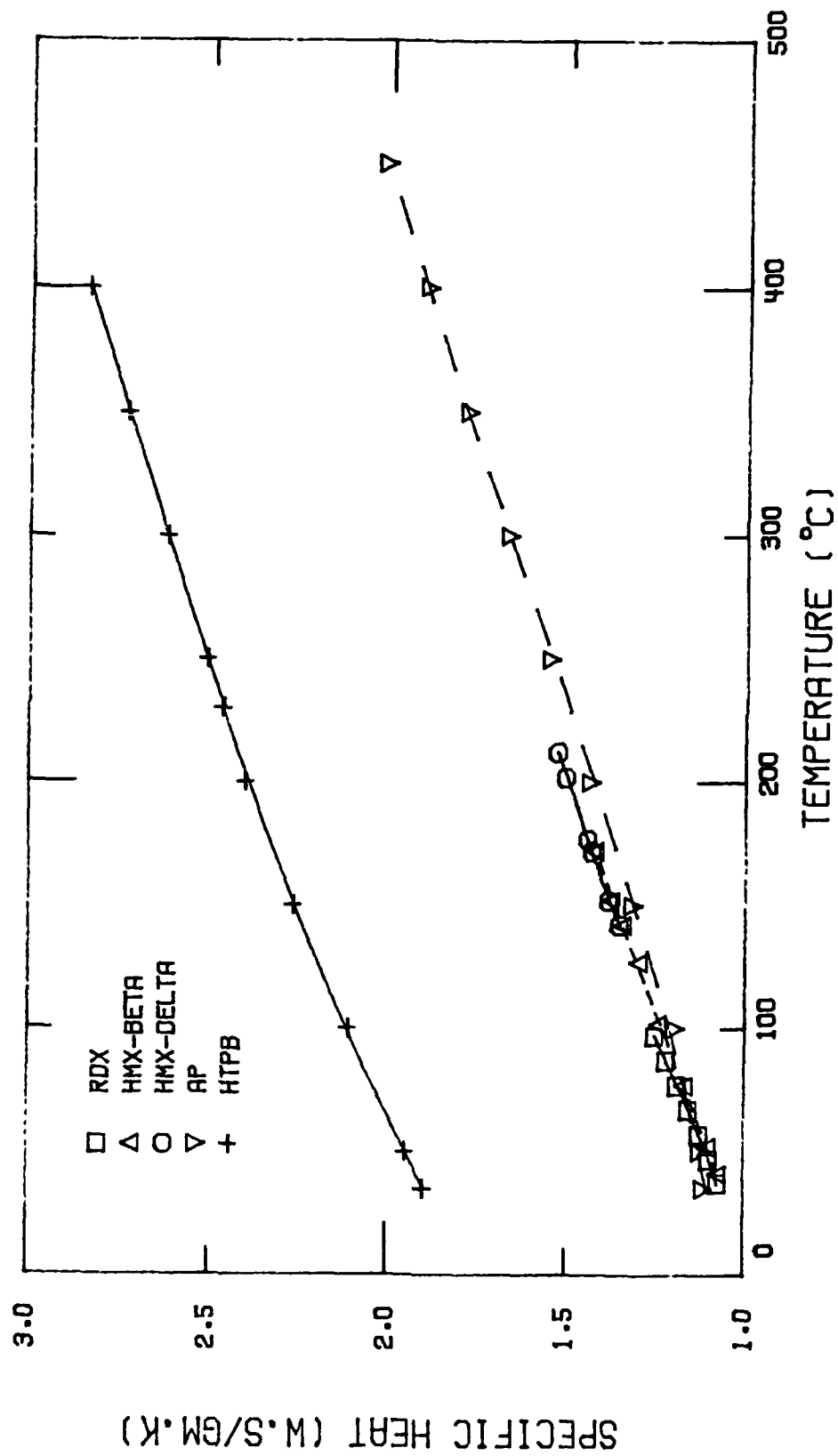
A cursory examination of the absorption coefficients as a function of wavelength for the energetic materials was made. This examination revealed the probability of significant radiant energy transmission into a unshielded sample from the laser ($1.06\ \mu\text{m}$) and of significant internal viewing of the sample by the IR detector. Therefore, only shielded samples were used; that is either samples left in the cups used to press them, or samples with a graphite disk attached to their front surfaces. The rear surfaces of all samples were spray-painted with a thin layer of black enamel to prevent the IR detector from viewing into the samples' interiors. Tests were conducted which showed that the spray-painting did not adversely affect the results. For these techniques a detailed study of the optical properties was not required. However, if we had pursued the strip-heating method, we would have had to account for radiation effects from the heater and this would have added formidably to the problems associated with this technique.

3.1 d Specific Heat

Specific heat measurements were made on single crystals of HMX and AP and on compacted samples of HMX, RDX and HTPB. The results are described in detail in a special report (TPRL 314), a publication and a thesis (see Appendix I). Values were obtained on pure and partially decomposed samples using several different heating rates. It was found that measured specific heat values were not significantly influenced by phase changes, the presence of decomposition products or heating rates. These results were expected from thermodynamic considerations (Law of DuLong and Petit and the Kopp-Neumann relationship). Typical results are plotted in Figure 4 and are tabulated in Appendix II. The present specific heat results for Beta HMX are in good agreement with Krien [15], Rylance [16], Velicky [6] and Wilcox [17]. The present values for Delta HMX are in good agreement with Rylance [16], but are in poor agreement with Krein [15]. Our values for RDX are in good agreement with Baytos [18] and Wilcox [17], but are somewhat lower than those for Velicky [6], at higher temperatures. The present values for AP are in good agreement with the JANNAF tables and Westrum [19]. A word of caution is in order. The specific heat values given here are useful for converting thermal diffusivity values to conductivity values. Of course, one will not obtain the correct total enthalpy of the system by integrating these specific heat values since the heats of transformations and decompositions are not included.

3.1 e Thermal Diffusivity

Thermal diffusivity values measured on AP single crystals are plotted in Figure 5. These results are for three samples in the $\langle 210 \rangle$ direction and two samples in each of the $\langle 2\bar{1}0 \rangle$ and $\langle 002 \rangle$ directions. These results show that the diffusivity in all three directions are essentially the same. These data also show the decrease in diffusivity values which occurs during the phase change and decomposition.



TEMPERATURE (°C)

Figure 4. Specific Heat

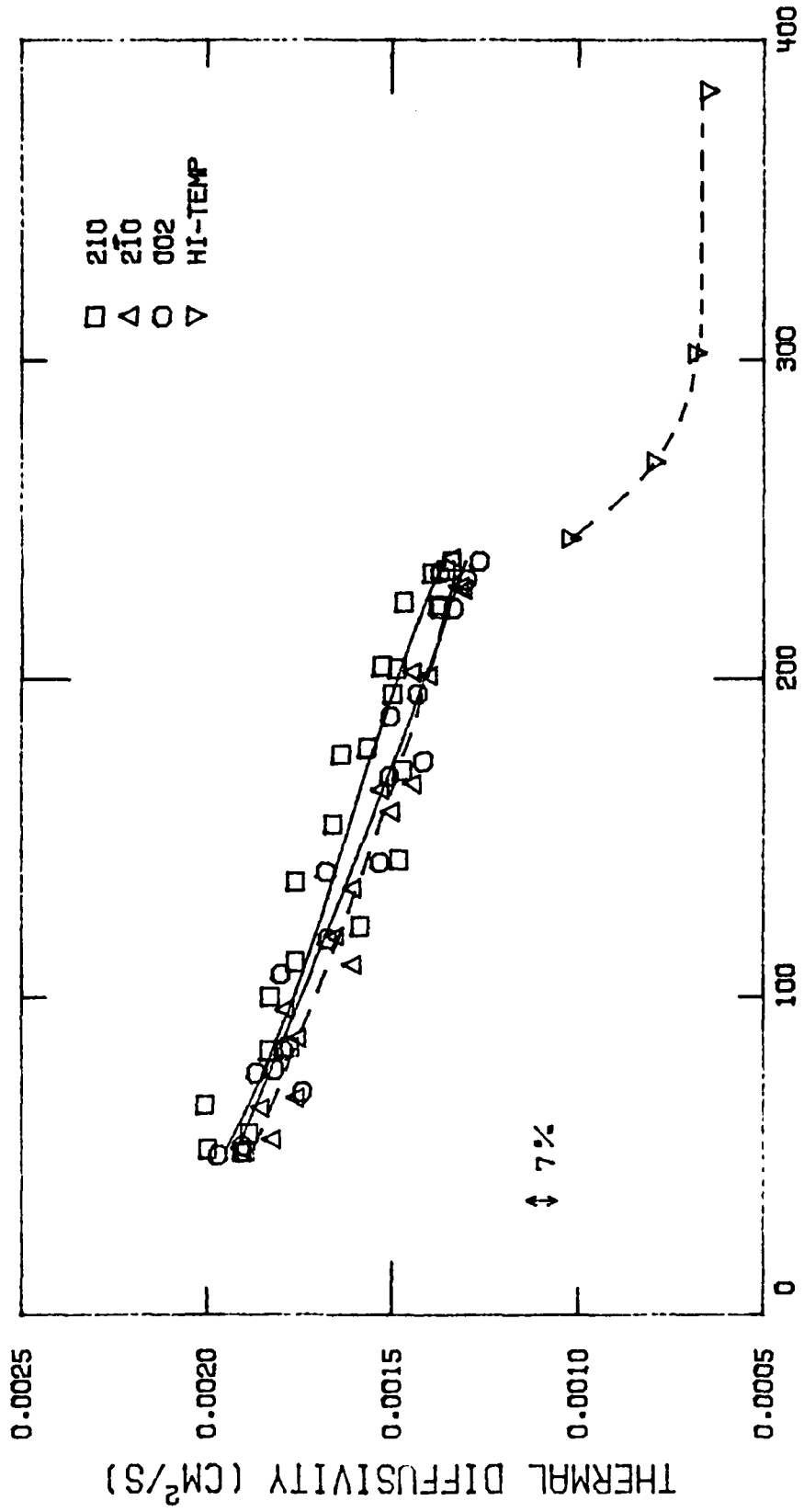


Figure 5. Thermal Diffusivity of AP Single Crystal

Thermal diffusivity results for HTPB binder and for various mixtures of HTPB and AP are plotted in Figure 6. These data show the relatively low values for HTPB and the increase in diffusivity values resulting from increasing percentages of AP. Included in Figure 6 are diffusivity values measured on two pressed powder samples. These samples were quite fragile. In fact, measurements could only be made on two specimens as the others did not survive transportation and handling. It is obvious that the values for the pressed powder samples are much lower than those for single crystals and that values measured on different samples vary significantly. Also shown in Figure 6 are the data on pressed powder by Parr and Parr [20] and Rosser, et al. [21].

Measurements on HMX were limited to pressed powder. Most measurements were made in SS/teflon cups, but some measurements were made on samples by gluing a graphite layer onto the front surface. The diffusivity values for HMX-2 are shown in Figure 7. While the sample was held at 187°C for about 40 minutes the diffusivity values decreased linearly with time and remained near the lower values during cooling. The behavior of the diffusivity values were similar for all the HMX samples but the magnitude of the values in the Beta phase varied from sample to sample, typical for pressed samples, especially those which have been transported large distances and subjected to mechanical vibrations. Values in the Delta phase for reacted samples were normally close together and were essentially temperature independent. Typical results are shown in Figure 8. Also included in the figure are the results of Parr and Parr [20].

Thermal diffusivity results on three pressed powder samples of RDX are shown in Figure 9. Also shown are the averaged, smoothed results of Faubion [22]. While the present values are significantly larger than those of Faubion, it is probable that the diffusivity values of single crystal RDX would be much larger than the values measured on pressed powder.

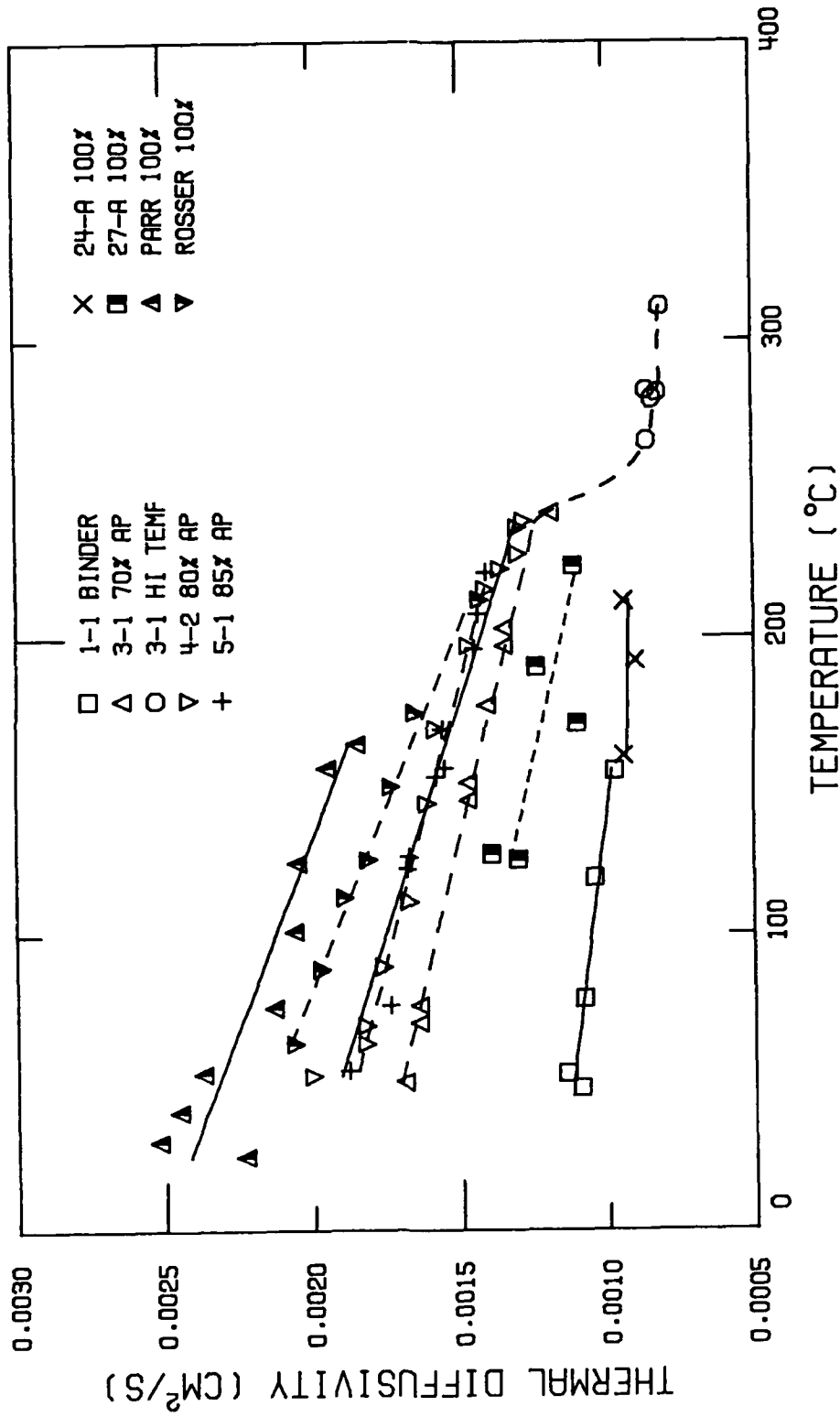


Figure 6. Thermal Diffusivity of AP/HTPB

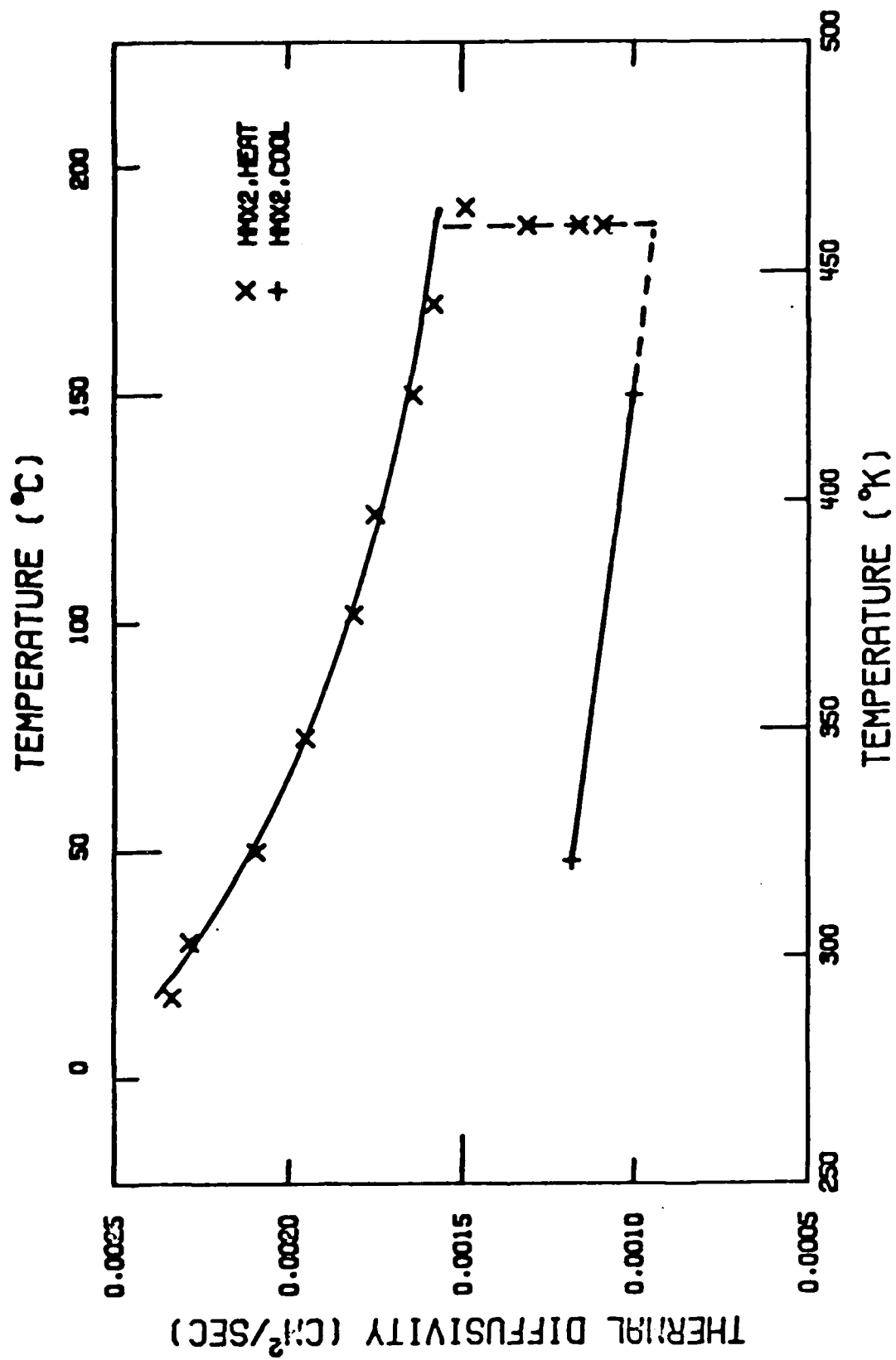


Figure 7. Thermal Diffusivity of HMX-2

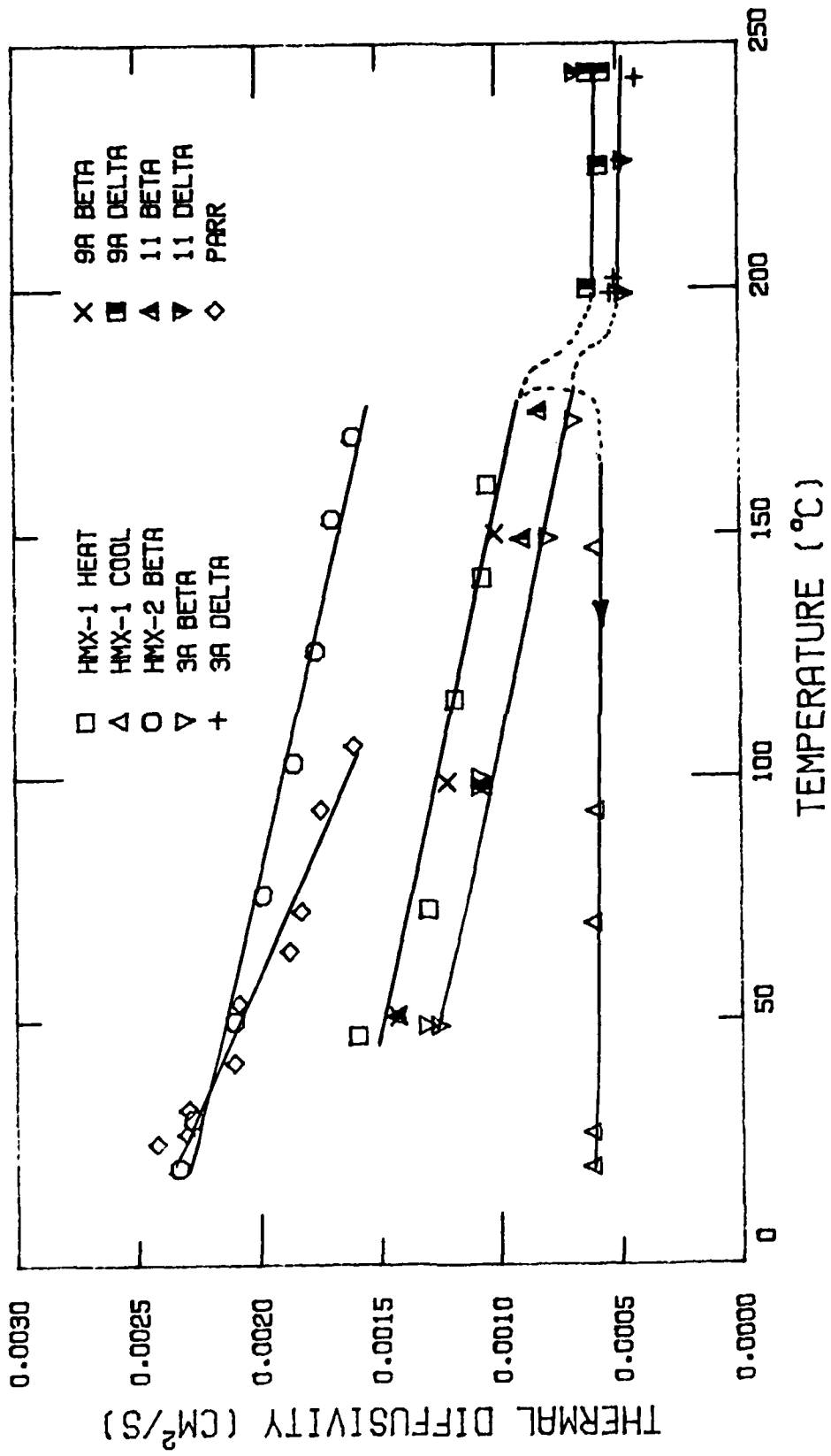


Figure 8. Thermal Diffusivity of HMX

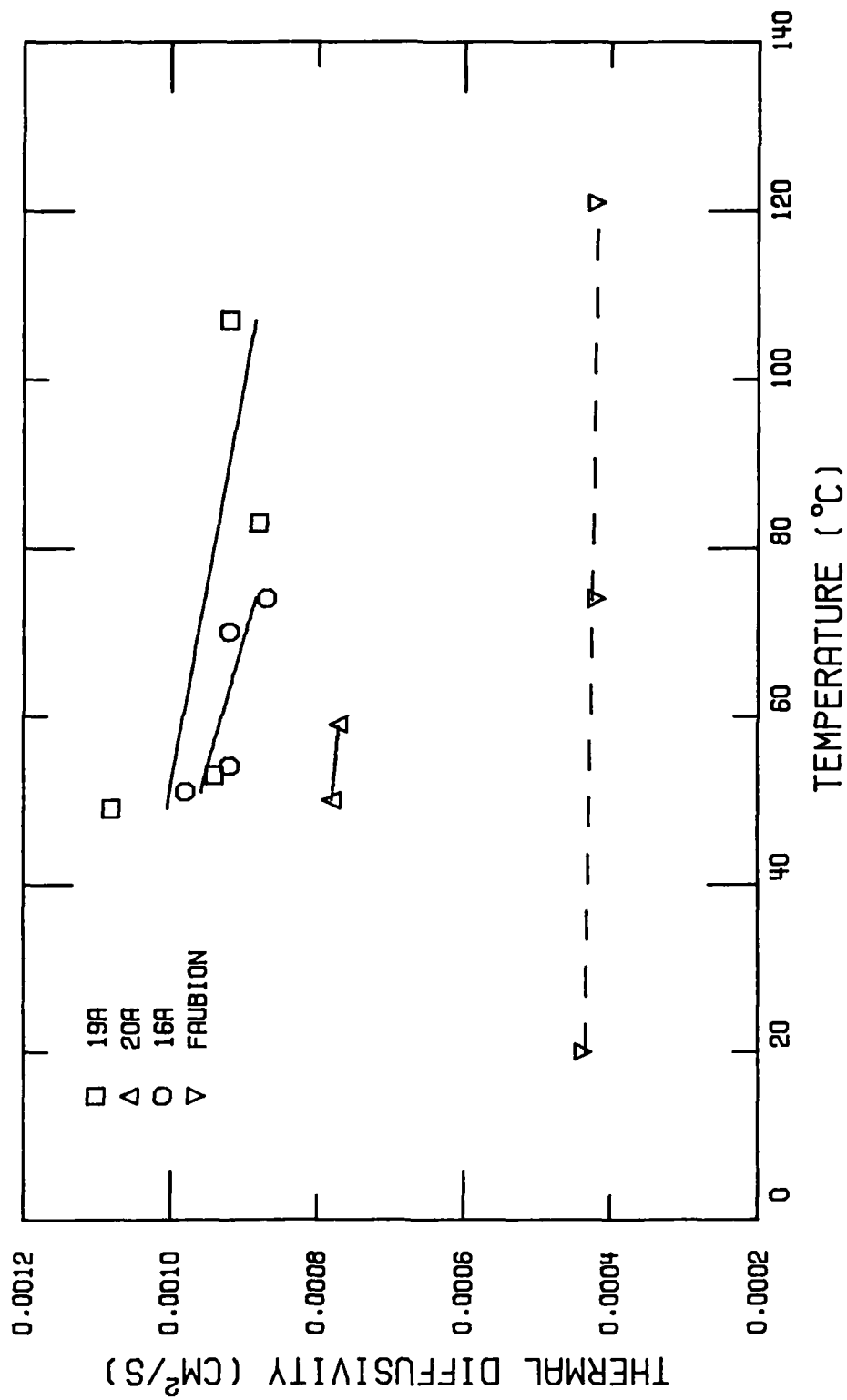


Figure 9. Thermal Diffusivity of RDX

3.1 f Thermal Conductivity

Thermal conductivity values for single crystal AP are calculated from the diffusivity data of Figure 5 and are shown in Figure 10.

Figure 11 shows the bulk conductivity values for the AP binder samples calculated using the diffusivities from Figure 6. Since the AP granules were much smaller than the sample thickness, the mixture can be treated as macroscopically homogeneous to enable calculation of these effective bulk conductivities, which represent only the precise mixtures measured.

To obtain conductivity values for pure AP from the mixture data available, an equation was required which relates the conductivities of each of the two strictly homogeneous phases in a mixture to the bulk conductivity of the mixture. Many relationships are available for this purpose [23]. The Russell equation was shown by Cheng and Vachon [24] to predict well the measurements of mixtures similar to the AP binder samples studied here. This model assumes that one of the two phases present is continuous, and the other is made up of discrete particles dispersed throughout the continuous medium. The Russell equation is

$$k_m = k_c \left[\frac{P_d^{2/3} + \frac{k_c}{k_d} (1 - P_d)^{2/3}}{P_d^{2/3} - P_d + \frac{k_c}{k_d} (P_d + 1 + P_d^{2/3})} \right]$$

where k_m is the mixture bulk conductivity, k_c is the conductivity of the continuous phase, k_d is the conductivity of the discontinuous phase and P_d is the volume fraction of the discontinuous phase.

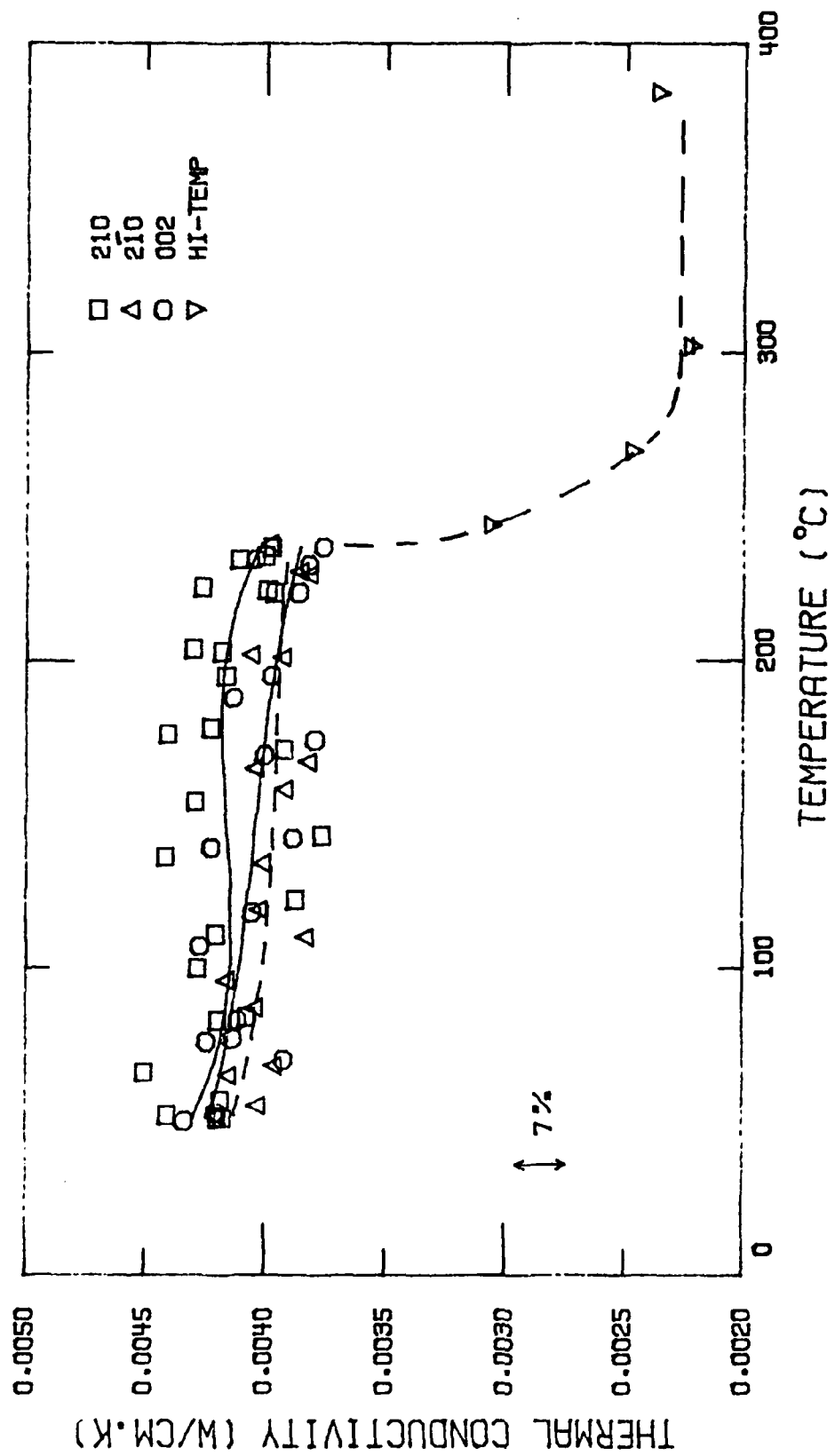


Figure 10. Thermal Conductivity of Single Crystal AP

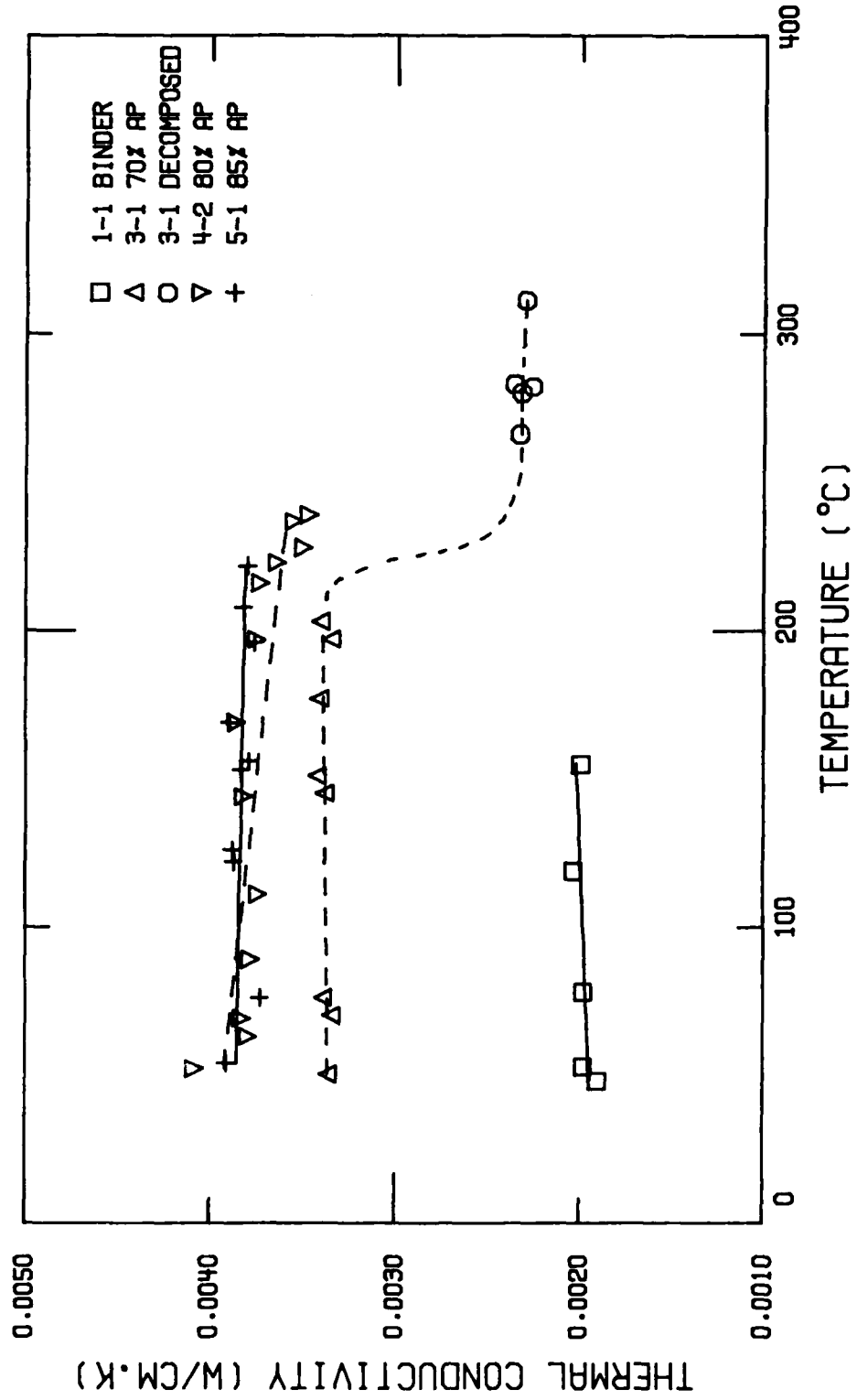


Figure 11. Thermal Conductivity of AP/HTPB

In applying equation (1) to the AP/binder samples, k_m was the measured values (from Figure 11), k_c was the binder conductivity (assumed to be constant at $0.00202 \text{ W/cm-}^\circ\text{K}$), and k_d was the unknown AP crystal conductivity. An iterative solution was implemented which provided the results shown in Figure 12 as pure crystal conductivities (average values for random directions through the crystal). Notice that samples with AP mass fractions between 70% and 85% provided essentially the same curve of calculated pure AP conductivity. The conductivity results for AP are summarized in Figure 13 which shows the average values for single crystals, the average values obtained from AP/HTPB mixture measurements and the results of Rosser, et al. [21] and Parr and Parr [20]. The results for the large single crystals are lower than those for small grain powders and this is thought to be due to lattice plane dislocations.

The diffusivity values of Figure 8 for HMX-2 in the Beta phase and for other samples in the Delta phase have been converted to conductivity values in Figure 14. Also shown in Figure 14 are the results of Parr and Parr [20]. All of these results, unfortunately, are for pressed powders. Single crystals of suitable HMX are not likely to be available in the near future. It is likely that the conductivity of HMX crystals in the Beta phase are significantly larger (up to 20% larger than HMX-2 Beta phase data). In retrospect, better values for the Beta phase material could be obtained by the method of mixtures as we applied to AP. In fact, a value for Beta HMX obtained by this method by Cornell and Johnson [25], is included in Figure 14. The method of mixtures would be very difficult to use for the Delta phase. Fortunately, the conductivity values in the Delta phase and molten region are not likely to be very different from the values obtained during the present work.

Thermal conductivity values for compacted powder for RDX are shown in Figure 15 and are compared to those of Faubion [22]. Remarks similar to those made for HMX apply to the RDX results.

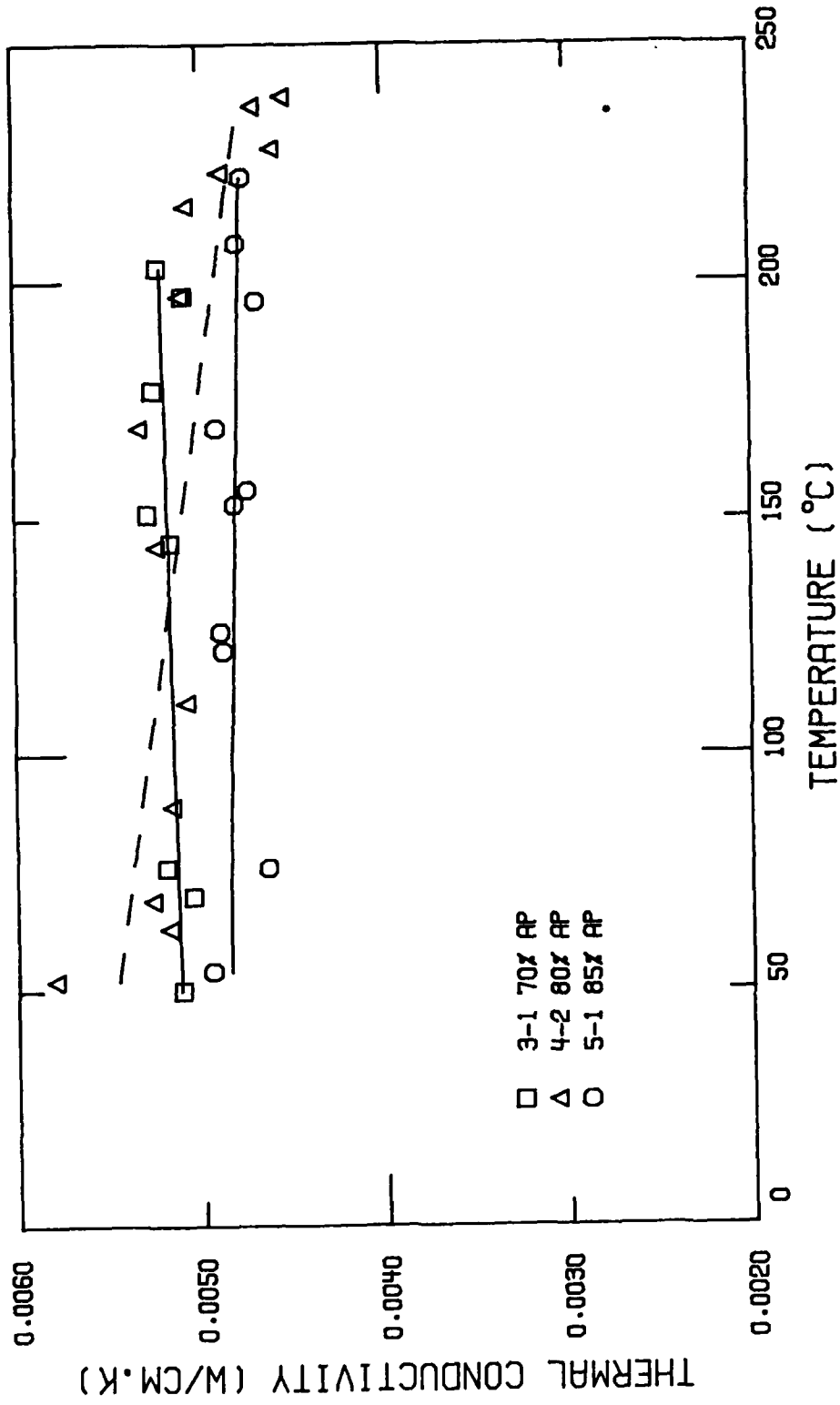


Figure 12. Thermal Conductivity of AP Calculated

from AP/HTPB Data

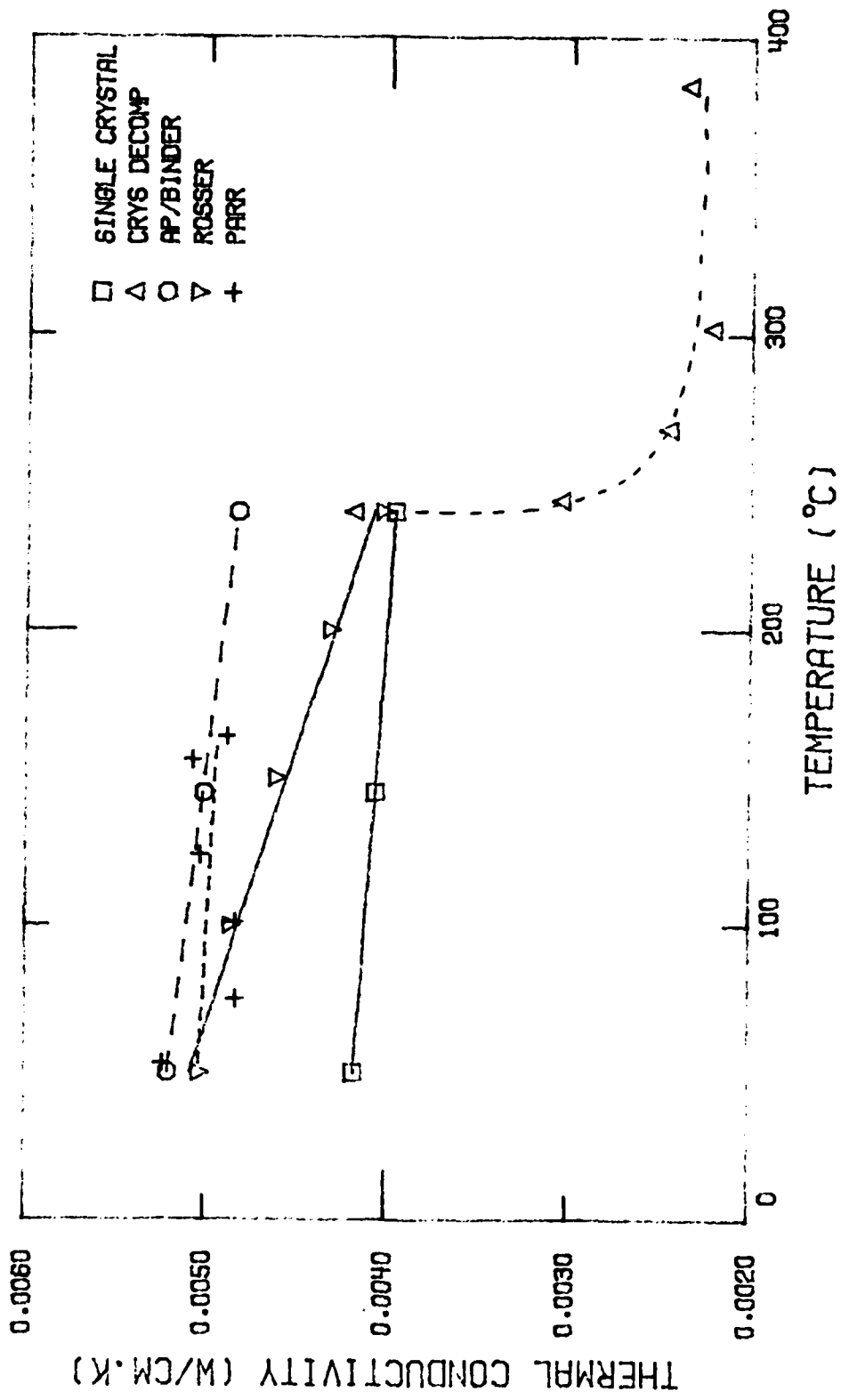


Figure 13. Thermal Conductivity of AP

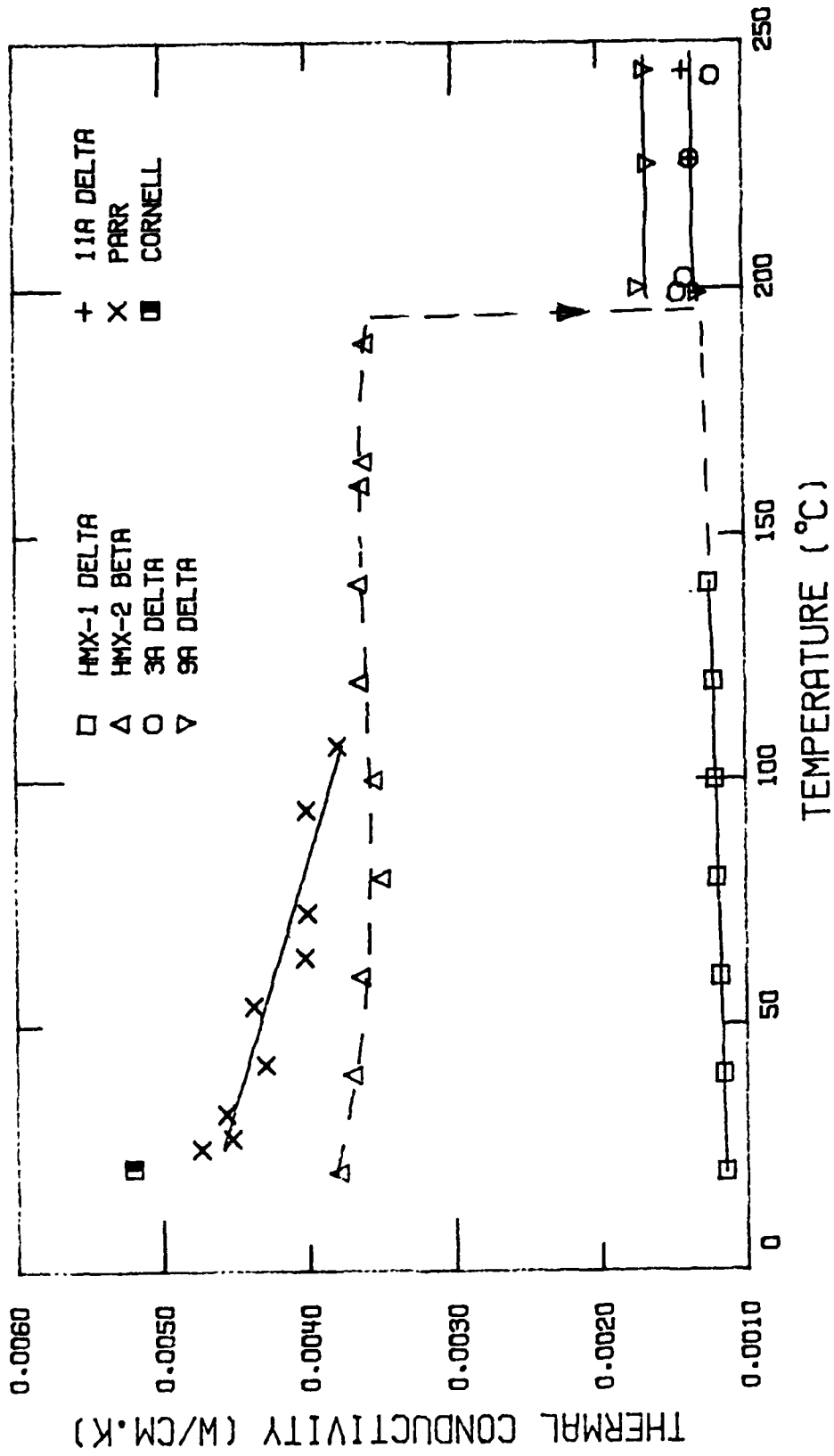


Figure 14. Thermal Conductivity of HMX

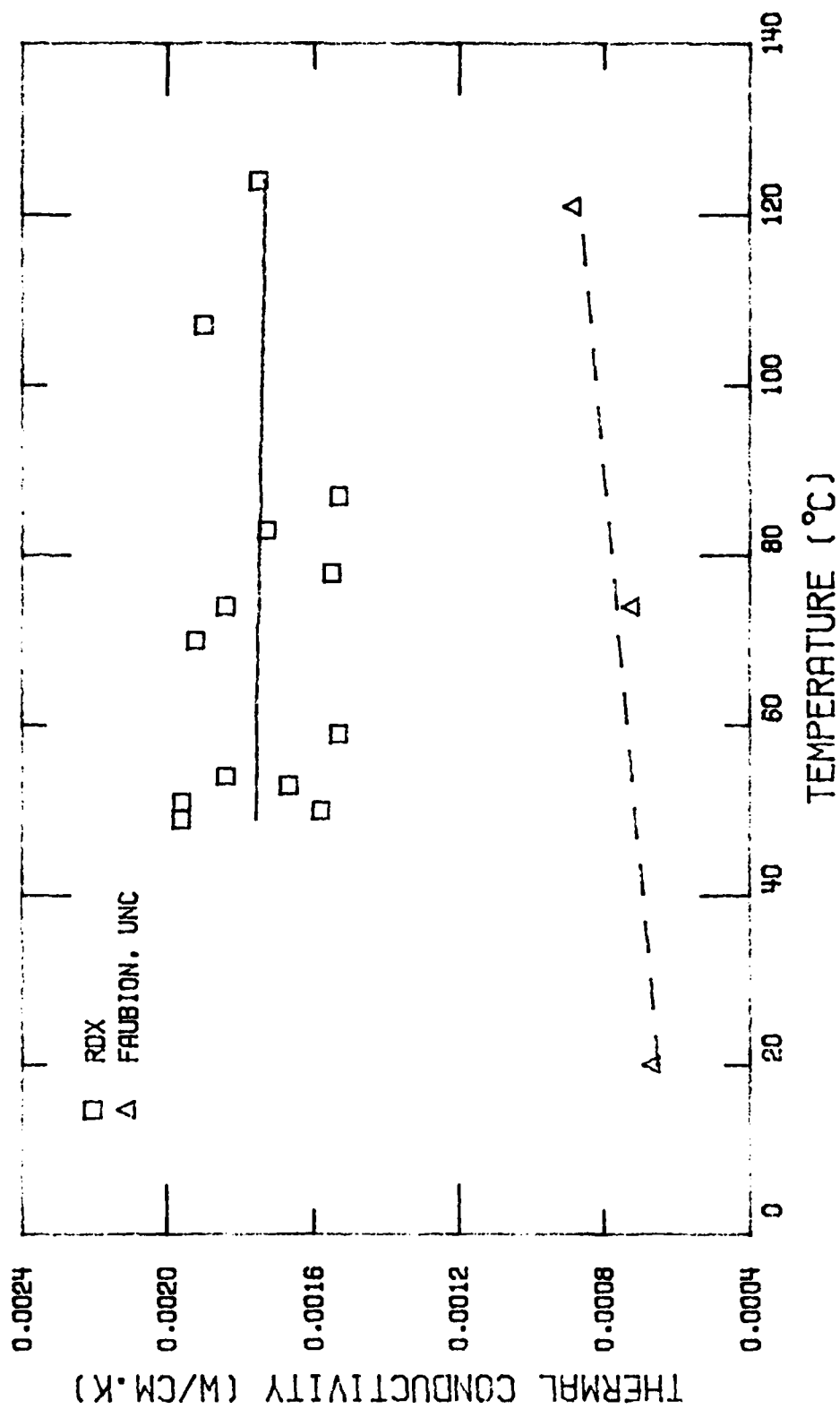


Figure 15. Thermal Conductivity of RDX

3.2 Carbon/Carbon Materials

The results of the research on transient heat flow in c/c materials have been extensively reported (see Appendix) so only the highlights will be summarized here. These highlights include the first demonstration of techniques to obtain in-situ diffusivity/conductivity values of carbon fibers in c/c and the first demonstration of the value of off-axis testing for unambiguous on-axis diffusivity/conductivity values. The computer output for the fiber-bundle experiment is given as Table 8. This output shows the thermal diffusivity of the in-situ fibers to be $2.79 \pm 0.05 \text{ cm}^2 \text{ sec}^{-1}$ at 23°C . The on-line comparison between theory and experiment of the rear face temperature rise of a sample machined at 45° to the axial and circumferential directions is shown as Figure 16. This remarkable agreement demonstrates the advantages of off-axis testing since such agreement cannot be obtained during on-axis tests. From the unambiguous off-axis results, the effective diffusivity values on-axis can be calculated. In addition, on-axis tests reveal the relative roles of the fibers and matrix subject to transient heat fluxes. Surface areas near fiber bundles running perpendicular to the surface receiving the heat flux remain cooler than the surrounding matrix, whereas the reverse is true at the opposite surface on moderate size specimens. The existence of hot and cold spots on the surface will effect localized erosion during rocket firing.

4.0 DISCUSSION

4.1 Energetic Materials

4.1 a AP

The specific heat of AP can be considered to be reasonably well known. Thermal diffusivity experiments have been performed on relatively large single crystals, samples composed of small grains combined with various percents of HTPB binder and on pressed

TABLE 8

THERMAL DIFFUSIVITY VALUES FOR A FIBER BUNDLE EXPERIMENT

THERMAL DIFFUSIVITY

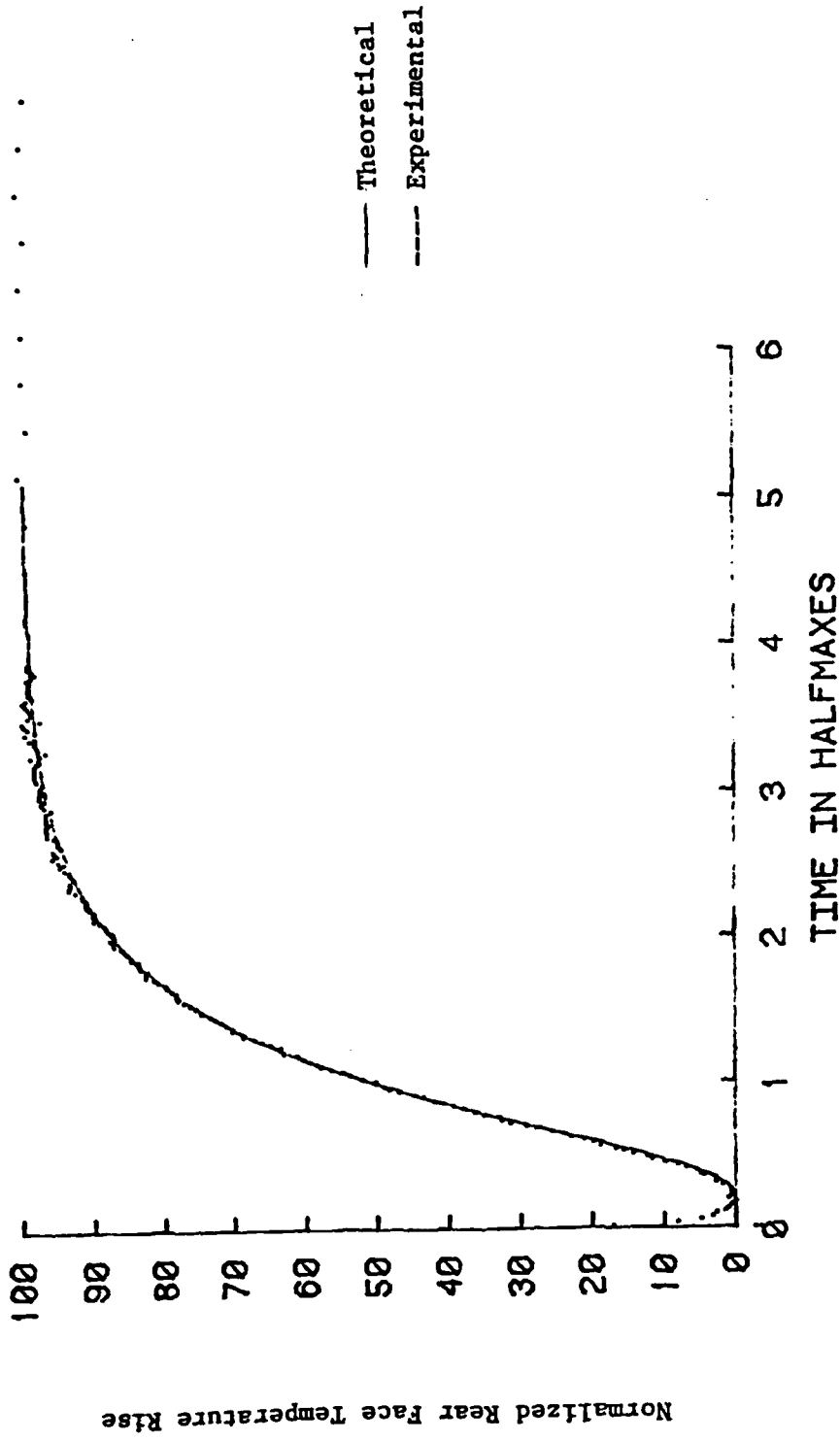
23C

	VALUE	TIME (SEC)
BASELINE:	0. 94000	0. 020680
HALFMAX:	3. 46995	0. 020033
MAXIMUM:	5. 99990	0. 073100

ALPHA	PERCENT	VALUE	TIME (SEC)
2. 68307	10. 0	1. 44599	0. 009761
2. 74091	20. 0	1. 95198	0. 012177
2. 75494	25. 0	2. 20498	0. 013333
2. 74287	30. 0	2. 45797	0. 014618
2. 72871	33. 3	2. 62663	0. 015530
2. 71593	40. 0	2. 96396	0. 017351
2. 74435	50. 0	3. 46995	0. 020033
2. 71226	60. 0	3. 97594	0. 023696
2. 74445	66. 7	4. 31327	0. 026136
2. 79052	70. 0	4. 48193	0. 027239
2. 82674	75. 0	4. 73493	0. 029499
2. 78008	80. 0	4. 98792	0. 033231
2. 82117	90. 0	5. 49391	0. 042620

FINITE PULSE TIME CORRECTION

2. 809385	25. 0
2. 776830	50. 0
2. 848231	75. 0



HALFTIME= 310996.9 MICROSECONDS
 BASELINE= 0.95000 VOLTS
 THICKNESS= 0.76450 CM

RUN ON 1/22/82
 UNFILTERED

Figure 16. NORMALIZED REAR FACE TEMPERATURE RISE FOR AXIAL-CIRCUMFERENTIAL SAMPLE AT 552°C.

powder. The results show that the conductivity in AP is essentially isotropic. Thermal conductivity values for AP calculated from the AP/binder data are about 20% larger than those for large single crystals, and this is probably due to lattice imperfections in the large crystals. It was necessary to cleave the crystals and it is known from x-ray studies that the crystals are easily damaged. The thermal conductivity values for AP in the orthorhombic phase between RT and 240°C should be considered to be $0.0050 \text{ Wcm}^{-1}\text{K}^{-1}$ (within 10%). The agreement of the present results with Parr and Parr [20] and Rosser, et al. [21] should be considered fortuitous since measurements made on pressed pellets usually yield much lower results than those for the individual grains themselves. The conductivity values for the cubic phase between 240°C and destruction/melting should be considered to be $0.0023 \text{ Wcm}^{-1}\text{K}^{-1}$. The values that could be obtained on pure, undamaged cubic AP crystals would undoubtedly be larger than this, but samples which have undergone phase transformation exhibit a great deal of imperfections. For purposes of modeling combustion in rocket motors with AP/HTPB fuel, the data of Figure 11 should be used. The values for Sample 3-1 after transformation should be used at all temperatures above 240°C.

4.1 b HMX and RDX

The specific heats of HMX in the Beta and Delta phases are well known. Thermal diffusivity experiments were performed only on pressed powders. Suitable single crystals were not available for diffusivity tests, although they were useful for specific heat. Thermal diffusivity values measured on pressed powders are undoubtedly lower than those for the individual grains so that the diffusivity of HMX is possibly about 20% above the values for HMX-2 shown in Figure 7. Since the conductivity of HMX/HTPB will be somewhat lower than that of good single crystal HMX, the conductivity values for HMX/HTPB will be close to those given in Figure 14 for HMX-2 in the Beta phase, and will decrease to the values shown in

Figure 14 for the Delta phase. The latter values should be applicable up to combustion.

The present values for the diffusivity and conductivity of RDX, while typical of pressed powders, are undoubtedly much lower than the values for individual grains. Reasonable values for grains will have to be obtained using samples containing known amounts of binder.

4.2 Carbon/Carbon Materials

The flash technique has been shown to be a powerful tool for studying transient heat flow in carbon/carbon materials. Using this technique it has been possible to obtain in-situ values for the fibers and the matrix, to study surface effects, to delineate the relative roles of the fibers and matrix and to explore directionality in an anisotropic media. The present work, combined with our earlier studies has revealed that the important values governing the diffusivity are:

- (1) Magnitude of diffusivity of fibers and of matrix,
- (2) fiber fraction ratio in direction of heat flow,
- (3) thickness of sample in relation to fiber bundle spacing and,
- (4) rear face temperature sampling area and location.

During the present program, the following items have been established:

- (1) It is possible to measure diffusivity values which correspond to thermal conductivity values by using a sufficiently thick sample and large viewing area. The sample thickness required becomes less as the temperature is increased.
- (2) It is possible to measure in-situ diffusivity values of fibers and of matrix by using point source temperature sensors and thin samples.
- (3) It is possible to determine the effects of imperfections such as delaminations on the thermal diffusivity. These effects are manifest by matrix values lower than those for regions where the defects are not present (point source detector methods) and by an increase in diffu-

sivity values for artifacts measured in gaseous environments as opposed to vacuum.

- (4) The nature of off-axis heat flow is beginning to be understood. The preliminary results are encouraging but are not completely internally consistent. The use of off-axis testing may be the best method for fully characterizing heat flow in 3-D material.
- (5) The tools to determine the skin depth in artifacts subjected to rapid heating have been developed. Beyond this surface layer the material may be treated as homogeneous for purposes of transient temperature response. For continuous heating this surface layer thickness is of the order of a yarn bundle spacing.
- (6) Within the surface layer there are substantial gradients in planes perpendicular to the heat flow (parallel to the surface). These may be of importance in ablation but are not necessarily important in bulk heat conduction.
- (7) The temperature of the fiber bundle near the surface is less than that of the surrounding matrix. At greater depths the difference goes through zero and then the bundles become hotter than the surrounding matrix.

5.0 SUMMARY AND CONCLUSIONS

The use of transient techniques to study the thermophysical properties of energetic materials and carbon/carbon composites used for rocket nozzles was explored. In the case of AP, transport data were obtained on single crystals, pressed powder and AP mixed with a binder. It was shown that the thermal conductivity and diffusivity of AP are essentially isotropic even in the orthorhombic phase. It was determined that the conductivity values for AP derived from the method of mixtures were superior even to the single crystal data due to defects in the large single crystals and that data on pressed samples led to low and variable results. The single crystal AP samples could have sustained some damage since they were six years old, had been transported over long distances and had been cleaved prior to being used for these measurements. The crystals appear to be fairly fragile and are hygroscopic. However, much effort was made to minimize damage to the crystals while in our possession. Conductivity values useful in both the orthorhombic phase (RT to about 240°C) and the cubic phase (240°C to melting) were obtained.

For HMX and RDX, transport properties were determined only on pressed powders. In the case of HMX, the largest conductivity values obtained in the Beta phase are probably about 20% lower than good single crystal values. However, in the Delta phase, the values should be representative up to the melting point. The conductivity values for RDX obtained on pressed powders are believed to be substantially low. It appears that pressing and transporting the RDX samples resulted in excessive damage to the pellets. For both HMX and RDX, it is recommended that future efforts concentrate on the method of mixtures method used for AP.

The study on transient effects in carbon/carbon materials was very productive. Successful techniques to obtain in-situ conductivity values for the fibers and matrix were successfully demonstrated for the first time and the relative roles of the fibers and matrix during transients were delineated. The remarkable advantages of off-axis testing were also revealed. It was shown that diffusivity values corresponding to steady state thermal conductivity could be obtained in carbon/carbon materials. However, it was also shown that there is a surface layer in which the interconstituent thermal gradients are significant and beyond which they are unimportant.

6.0 REFERENCES

- [1] Venkatesan, K., "The Crystal Structure of Ammonium Perchlorate - NH_4ClO_4 ", Proceedings of the Indiana Academy of Science, Vol. 46, 1957, p. 134.
- [2] Wyckoff, R.W.G., Crystal Structures, Vol. II, Interscience Pub., New York, 1960.
- [3] Henry, Norman F. and Lonsdale, Kathleen, ed., International Tables for X-ray Crystallography, Vol. I, The Keynoch Press, Birmingham, England, 1952.
- [4] Markowitz, M.M. and Boryta, D.A., "Some Aspects of the Crystallographic Transition of Ammonium Perchlorate", ARS Journal, Vol. 32, 1962, p. 1941.
- [5] Brill, T.B. and Goetz, F., "Laser Raman Study of the Thermal Decomposition of Solid NH_4ClO_4 ", Journal of Chemical Physics, Vol. 65, 1976, p. 1217.
- [6] Velicky, R., Lenchitz, C. and Beach, W., "Enthalpy Change, Heat of Fusion and Specific Heat of Basic Explosives", Picatinny Arsenal, Technical Rept. 2504, 1959.
- [7] Sergio, S.T., "Studies of the Polymorphs of RDX", Master's Thesis, Department of Chemistry, Delaware Univ., 1978.
- [8] Dobratz, B.M., "Properties of Chemical Explosives and Explosive Stimulants", Lawrence Livermore Laboratory, Rept. UCRL-51319, Rev. 1, 1972.
- [9] Brill, R.B. and Karpowicz, R.J., "Solid Phase Transition Kinetics: The Role of Intermolecular Forces in the Condensed Phase Decomposition of Octahydro - 1,3,5,7 - Tetranitro - 1,3, 5,7 - Tetrazocine (HMX)", J. Phys. Chem., Vol. 86, 1982, pp. 4260-4265.
- [10] Cady, H.H. and Smith, L.C., "Studies on the Polymorphs of HMX", Los Alamos Scientific Laboratory, Los Alamos, NM, LAMS-2652, May 1962.
- [11] Kraeutle, K.J., "The Thermal Decomposition of Orthorhombic Ammonium Perchlorate Single Crystals", Journal of Physical Chemistry, Vol. 74, 1970, P. 1350.
- [12] Jacobs, P.W.M. and Pearson, G.S., "Mechanism of the Decomposition of Ammonium Perchlorate", Combustion and Flame, Vol. 13, 1969, p. 419.

- [13] Ellis, R.A., "7-Inch Billet Program Progress Report", RNTS Meeting, 1979, CPIA Publication, 310, January 1980.
- [14] EMTL, "Interim Report on Mechanical and Thermal Properties of Billet F-11, Seven Inch Mantech Billet Program, Vol. II, Thermal Properties", MCIC, No. 109500, March 1980.
- [15] Krien, G., Licht, H.H. and Zierath, J., "Thermochemische Untersuchungen An Nitraminen", Thermochem. Acta, Vol. 6, 1973, pp. 465-472.
- [16] Rylance, J. and Stubley, D., "Heat Capacities and Phase Transitions of Octahydro - 1,3,5,7 - Tetranitro - 1,3,5,7 - Tetranitro - 1,3,5,7 - Tetrazocine (HMX)", Thermochem. Acta, Vol. 13, 1975, pp. 253-259.
- [17] Wilcox, J.D., "Differential Scanning Calorimetry Method in the Determination of Thermal Properties of Explosives," Air Force Institute of Technology, Air University, Wright-Patterson Air Force Base, OH, Master of Science Thesis, GAW/ME/67B-3, June 1967.
- [18] Baytos, John F., "Specific Heat and Thermal Conductivity of Explosives, Mixtures, and Plastic-Bonded Explosives Determined Experimentally", Los Alamos Scientific Laboratory, Informal Rept. LA-8034-MS.
- [19] Westrum, E.F. and Justice, B.H., "Molecular Freedom of the Ammonium Ion. Heat Capacity and Thermodynamic Properties of Ammonium Perchlorate from 5° - 350°K", Journal Chem Phys., 50, No. 12, June 1969
- [20] Parr, D.M. and Parr, T.P., "Condensed Phase Temperature Profiles in Deflagrating HMX", Unpublished, Naval Weapons Center.
- [21] Rosser, W.A., Inami, S.H. and Wise, H., "Thermal Diffusivity of Ammonium Perchlorate", AIAA Journal, Vol. 4, 1966, p. 663.
- [22] Faubion, B.D., "Thermal Conductivity of RDX", Sandia Laboratories, P.O. No. C3-5541, Nov. 1976.
- [23] Powers, A.E., "Conductivity in Aggregates", Proceedings of Second Conference on Thermal Conductivity, Ottawa, Ontario, 1962.

- [24] Cheng, S.C. and Vachon, P.I., "A Technique for Predicting the Thermal Conductivity of Suspension, Emulsions and Porous Materials", Int. Journal of Heat and Mass Transfer, Vol. 13, 1970, p. 537.
- [25] Cornell, R.H. and Johnson, G.L., "Measuring Thermal Diffusivities of High Explosives by the Flash Method", UCRC-52565, Oct. 23, 1978.

APPENDIX I

Publications, Presentations and Reports

Publications

1. "Variations in the Measurement of Thermal Diffusivity on Coarse-Weave Carbon/Carbon Composites in Terms of Fiber Fraction Involvement," Deshpande, M.S., Bogaard, R.H. and Taylor, R.E., International Journal of Thermophysics, 2(4), pp. 357-70, 1981.
2. "Thermophysical Properties of Fine-Weave Carbon/Carbon Composites," Taylor, R.E., Groot, H. and Shoemaker, R.L., Spacecraft Radiative Transfer and Temperature, 83, 96-108, AIAA, Progress in Astronautics and Aeronautics, T.E. Horton, Ed., 1982.
3. "Specific Heat of Octahydro-1,3,5,7-Tetranitro-1,3,5,7-Tetrazocine (HMX)," Koshigoe, L.G., Shoemaker, R.L. and Taylor, R.E., submitted to AIAA Journal, 1983.
4. "Thermal Diffusivity of Fiber-Reinforced Composites Using the Laser Flash Technique," Taylor, R.E., Jortner, J. and Groot, H., accepted for publication in CARBON, June 1984.
5. "Theory of Pulse Measurement of Thermal Diffusivity on Two-Layer Slabs," James, H.M., submitted to High Temperatures - High Pressures, June 1984.
6. "Measurement of Thermal Transport Properties of Selected Solid Rocket Propellant Components", Stark, J.A., Master of Science Thesis, School of Mechanical Engineering, Purdue University, August 1984.
7. "Determination of Thermal Transport Properties in Ammonium Perchlorate", Stark, J.A. and Taylor, R.E., in preparation for submission to AIAA Journal, July 1984.

Presentations

1. "On the Measurement of Thermal Diffusivity on Coarse-Weave C-C Composites and the Dependence upon Fiber Fraction", Deshpande, M.S., Bogaard, R.H. and Taylor, R.E., AIAA 16th Thermophysics Conference, June 1981, Palo Alto, CA.
2. "Thermophysical Properties of Fine Weave Carbon/Carbon Composites", Taylor, R.E., Groot, H. and Shoemaker, R.L., AIAA 16th Thermophysics Conference, June 1981, Palo Alto, CA.

3. "Thermal Diffusivity Measurements on HEPN", Taylor, R.E. and Groot, H., JANNAF Carbon/Carbon Rocket Nozzle Technology Meeting, Oct. 1981, Hampton, VA.
4. "Off Axis Thermal Diffusivity Testing of 3D Carbon-Carbon Composites", Jortner, J.J. and Taylor, R.E., 4th Carbon-Carbon Nozzle Technology Meeting, October 1982, Monterey, CA.
5. "Analysis of Transient Thermal Responses in a Carbon-Carbon Composite", Jortner, J.J., Symposium on Thermomechanical Behavior of High Temperature Composites, A.S.M.E., Nov. 1982, Phoenix, AZ.
6. "Thermal Diffusivity of Fiber-Reinforced Composites Using the Laser Flash Technique", Taylor, R.E. and Groot, H., 16th Biennial Conference on Carbon, Jul7 1983, San Diego, CA.
7. "Thermophysical Properties of Propellants", Shoemaker, R.L., Stark, J.A. and Taylor, R.E., 18th International Conductivity Conference, October 1983, Rapid City, S.D.

Reports

1. "Thermophysical Properties of a Carbon/Carbon Composite", Special Report to AFOSR Grant 77-3280, (TPRL 244), May 1981, R.E. Taylor and H. Groot.
2. "Thermal Diffusion in Carbon/Carbon Composites", Report to AFOSR (TPRL 256), February 1982, R.E. Taylor and H. Groot.
3. "Thermophysical Property Determinations Using Transient Techniques", Annual Report to AFOSR (TPRL 280), March 1982, R.E. Taylor, R.L. Shoemaker and L.G. Koshigoe.
4. "Analysis of Transient Temperature Response in a Carbon-Carbon Composite During Flash-Method Thermal Diffusivity Test", J.J. Jortner, Issue no. 12, Current Awareness Bulletin, published by Metal and Ceramics Information Center, Battelle Columbus Labs, August 1981.
5. "Coarse Weave C-C Composites: A Viewing Spot Size Problem Occurring for Thermal Diffusivity Specimen", M.S. Desphande, R.H. Bogaard and R.E. Taylor, Issue No. 11, Current Awareness Bulletin, published by Metal and Ceramics Information Center, Battelle Columbus Labs, April 1981.
6. "Analysis of Transient Temperature Response of a Carbon-Carbon Composite During Continuous Heating at One Surface", J.J. Jortner, supplement to TPRL 256, February 1982.

7. "On the Use of Off-Axis Testing to Characterize the Thermal Diffusivities of Orthogonally Reinforced Carbon-Carbon Composites", J.J. Jortner, supplement to TPRL 256, February 1982.
8. "Strip Heating Method, Analysis and Conclusions Based on the Results from Preliminary Measurement", (TPRL 300), A. Dobrosavljevic and J.A. Stark, July 1982.
9. "Specific Heat of Octahydro-1,3,5,7-Tetranitro-1,3,5,7-Tetrazocine (HMX)", Special Report to AFOSR (TPRL 314), January 1983, L.G. Koshigoe, R.L. Shoemaker and R.E. Taylor.
10. "Specific Heat of Octahydro-1,3,5,7-Tetranitro-1,3,5,7-Tetrazocine (HMX)", Special Report to AFOSR (TPRL 314A), October 1983, L.G. Koshigoe, R.L. Shoemaker and R.E. Taylor.
11. "Thermophysical Property Determinations Using Transient Techniques", Annual Report to AFOSR (TPRL 327), April 1983, R.E. Taylor, R.L. Shoemaker and L.G. Koshigoe.

APPENDIX II. Tabulated Values

Table A1. Data plotted in Figure 4

Temperature (°C)	Specific Heat (J/g-K)	Material
37	1.073	RDX
47	1.098	RDX
57	1.125	RDX
67	1.155	RDX
77	1.186	RDX
87	1.218	RDX
97	1.251	RDX
41	1.073	HMX-Beta
52	1.102	HMX-Beta
77	1.167	HMX-Beta
102	1.241	HMX-Beta
127	1.298	HMX-Beta
142	1.341	HMX-Beta
152	1.374	HMX-Beta
172	1.419	HMX-Beta
142	1.349	HMX-Delta
152	1.381	HMX-Delta
172	1.429	HMX-Delta
177	1.439	HMX-Delta
202	1.501	HMX-Delta
212	1.522	HMX-Delta
35	1.113	AP
50	1.123	AP
100	1.196	AP
150	1.314	AP
200	1.431	AP
250	1.547	AP
300	1.664	AP
350	1.781	AP
400	1.898	AP
450	2.014	AP
35	1.895	HTPB
50	1.945	HTPB
100	2.109	HTPB
150	2.263	HTPB
200	2.397	HTPB
230	2.461	HTPB
250	2.506	HTPB
300	2.617	HTPB
350	2.729	HTPB
400	2.840	HTPB

Table A2. Data plotted in Figure 5

Temperature (°C)	Diffusivity (cm ² /s)	Sample (No.) Direction < >	Temperature (°C)	Diffusivity (cm ² /s)	Sample (No.) Direction < >
51	0.001893	2-5 <210>	76	0.001864	3-5 <002>
122	0.001585		107	0.001798	
143	0.001479		139	0.001674	
171	0.001470		169	0.001504	
195	0.001498		188	0.001505	
223	0.001373		222	0.001332	
237	0.001337		237	0.001265	
57	0.001882	2-8 <210>	50	0.001968	3-6 <002>
84	0.001772		53	0.001901	
100	0.001828		77	0.001813	
136	0.001757		70	0.001740	
176	0.001634		83	0.001792	
204	0.001526		118	0.001672	
222	0.001367		142	0.001529	
234	0.001353		174	0.001413	
51	0.001902	3-2 <210>	231	0.001298	
52	0.001995		233	0.001370	
66	0.002003		195	0.001430	
83	0.001829				
111	0.001757		244	0.001018	Hi-Temp <210>
154	0.001656		268	0.000792	
178	0.001565		302	0.000680	
203	0.001484		384	0.000648	
224	0.001465				
233	0.001392				
52	0.001907	3-3 < $\bar{2}10$ >			
55	0.001822				
65	0.001852				
110	0.001605				
134	0.001605				
167	0.001443				
202	0.001445				
228	0.001305				
238	0.001305				
68	0.001758	3-4 < $\bar{2}10$ >			
87	0.001752				
96	0.001787				
119	0.001653				
158	0.001502				
165	0.001530				
201	0.001401				
229	0.001317				